

# **Pilot scale degradation study of 16 selected volatile organic compounds by hydroxyl and sulfate radical based Advanced Oxidation Processes**

*André Fernandes<sup>1</sup>, Patrycja Makoś<sup>1</sup>, Javed Ali Khan<sup>2</sup>, Grzegorz Boczkaj<sup>1,\*</sup>*

<sup>1</sup>Gdansk University of Technology, Faculty of Chemistry, Department of Chemical and Process Engineering, 80 – 233 Gdansk, G. Narutowicza St. 11/12, Poland

<sup>2</sup>Radiation Chemistry Laboratory, National Centre of Excellence in Physical Chemistry, University of Peshawar, Peshawar 25120, Pakistan

*\* Corresponding author: Dr Grzegorz Boczkaj, PhD. Sc. Eng. Fax: (+48 58) 347-26-94; Tel: (+48) 697970303; E-mail: grzegorz.boczkaj@gmail.com or*

*grzegorz.boczkaj@pg.edu.pl*

Postprint of: Fernandes A., Makoś P., Khan J., Boczkaj G.: Pilot scale degradation study of 16 selected volatile organic compounds by hydroxyl and sulfate radical based advanced oxidation processes. JOURNAL OF CLEANER PRODUCTION. Vol. 208, (2019), pp. 54-64. DOI: 10.1016/j.jclepro.2018.10.081

## Abstract

The studies of effective technologies for complete degradation of the volatile organic compounds (VOCs), are very important due to the high biotoxicity of the VOCs which makes the biological technologies ineffective. It also increases the risk of VOCs emission instead of their treatment when using open air biological technologies. In the present study, different types of Advanced Oxidation Processes (AOPs) were investigated for the degradation of several VOCs in a model pilot scale effluent, simulating effluents from bitumen production. The goal of this paper is to reach effective VOCs and wastewater degradation to make the bitumen production a cleaner process.  $O_3$ ,  $H_2O_2$ ,  $O_3/H_2O_2$  (the so called peroxone), persulfate (PS) and peroxymonosulfate (PMS) were processes chosen for this work. Heat activation enhanced the total VOCs degradation in PS and PMS technologies, which achieved higher effectiveness than  $H_2O_2$ . Peroxone process at 40 °C achieved the highest efficiency of all processes studied needing only 60 min to completely degrade all compounds without any oxidation by-products. Sulfur containing VOCs (VSCs) were completely degraded in a shorter treatment time and nitrogen containing VOCs (VNCs) needed more time of treatment in all technologies studied. The preference of the hydroxyl and sulfate radicals for degradation of oxygen containing VOCs (O-VOCs) had different behavior depending on the group of compounds and should be considered in future research for combined radical processes.

**Keywords:** VOCs degradation; wastewater treatment; hydroxyl radicals; sulfate radicals; GC-MS; AOPs



## 1. Introduction

Volatile Organic Compounds (VOCs) represent a group of compounds that are known to need special precautions when choosing a targeted treatment. They are widely present in several types of industrial facilities, as raw materials or as by-products or as waste (Kim and Hong, 2002). Due to their carcinogenic nature, some VOCs are considered to be harmful to human health, other animals, plants and microorganisms present in the environment (Cheng and Hsieh, 2013; Ren et al., 2018). The discharge limits of each of the VOCs may depend on the country and have been decreasing in the last years (Boczkaj et al., 2010; Ojala et al., 2011). There are several types of VOCs, including oxygen containing volatile organic compounds (O-VOCs), sulfur containing VOCs (VSCs) and nitrogen containing VOCs (VNCs) (Boczkaj et al., 2014). VOCs origin depends on the type of industrial facility, which can be pharmaceutical (Li et al., 2014), dyes (Ning et al., 2015), cellulose (Rigol et al., 2002) or petroleum refinery (Cheng and Hsieh, 2013; Stepnowski et al., 2002). These types of industries are investing significantly in the last years in researching and developing strategies to treat their wastewater (WW). The idea all along is to reuse part of the WW generated with the anticipation of environmental sustainability and control over fresh water shortage. Elimination of VOCs from industrial effluents could be one of the big steps contributing to the aforementioned desire of WW reuse. To effectively degrade VOCs, there is a need to choose an appropriate technology to avoid their emission to the atmosphere. Some of the VOCs have complex structures, like aromatics and poly-aromatics, which are not degraded by the biological approach. Some studies already attempted the combination of Advanced Oxidation Processes (AOPs) and biological technologies to reach effective treatment of heavy polluted effluents and, therefore, reaching cleaner production (Bahri et al., 2018). Effluents like spent caustic (Hariz et al., 2013; Oh and



Shin, 2013), petroleum & refinery (Saien and Nejati, 2007; Saïen and Shahrezaei, 2012), bitumen (Autelitano and Giuliani, 2018; Ventura et al., 2015), post oxidative effluents from bitumen production (Boczkaj et al., 2010, 2014) are examples of caustic effluents that need special precaution when treated.

Degradation of VOCs has widely been studied by different types of remediation technologies with the investigation of all parameters affecting the technology efficiency. Nevertheless, studies are focused on a model WW containing one compound, and the effect of a second pollutant present in the model WW. To fully analyze the effectiveness of studied processes, the research should include studies using a model WW containing several VOCs for evaluation of the total effect of treatment using scenario that simulates as much real effluents as possible. Some studies have used the above approach by preparing a model WW containing several types of VOCs (Goel et al., 2004; Shen and Ku, 1999; Wols et al., 2013). Previous studies on the treatment of effluents from bitumen production by hydroxyl radical based advanced oxidation processes (H-AOPs) and sulfate radical based AOPs (S-AOPs) revealed partial decrease of the chemical oxygen demand (COD), around 45%. The particular groups of compounds responsible for the low COD reduction have been reported to be saturated hydrocarbons (Boczkaj et al., 2017; Fernandes et al., 2018). Thus, the model WW was prepared to understand if the selected conditions on the real effluents studies are effective for the certain groups of compounds. In addition, it is important to understand if their degradation behavior is the same as the VOCs present in the real effluents and if they can produce harmful by-products which can be one of the hypothesis of the partial COD reduction in previous work (Boczkaj et al., 2017). Thus, the processes and operational parameters studied in this work were the same as previous papers mentioned above.



AOPs were first reported by Glaze, who stated that AOPs are capable for generation of highly reactive species named hydroxyl radicals ( $\text{HO}^\bullet$ ) (Glaze and Kangt, 1989).  $\text{HO}^\bullet$ , possesses a high oxidation potential ( $E^\circ = 2.7 \text{ V}$ ), is capable of oxidizing the majority of the organic compounds (Litter, 2005; Shahidi et al., 2015; Ali et al., 2018). In some cases, the compounds can be fully mineralized to  $\text{CO}_2$  and  $\text{H}_2\text{O}$ . In the recent decades, new technologies inside the AOPs technology had emerged, based on the use of persulfate (PS) and peroxymonosulfate (PMS) as oxidants, the so called S-AOPs (Khan et al., 2013; 2014; 2017). Usually PMS is available either pure or as a triple salt ( $2\text{KHSO}_5 \cdot \text{KHSO}_4 \cdot \text{K}_2\text{SO}_4$ ) called Oxone (Sharma et al., 2015). These processes are known to generate sulfate radicals ( $\text{SO}_4^{\bullet-}$ ) with high oxidation potential ( $E^\circ = 2.6 \text{ V}$ ) similar to  $\text{HO}^\bullet$  (Ghanbari et al., 2016; Matzek and Carter, 2016). These technologies possess a wider working pH range than classic AOPs (i.e., H-AOPs) and can be more effective for treatment of caustic effluents (Boczka and Fernandes, 2017).

The goal of this paper is to simulate a strong alkaline model WW, containing several VOCs, to check their degradation behavior using the same AOP technologies used in previous studies with real effluents (Boczka et al., 2017; Fernandes et al., 2018). Also the study of the by-products of oxidation will help understand if there are any toxic and harmful by-products produced during oxidation of the model WW. This model effluent should simulate as much as possible the caustic effluents from refinery industries, namely, post oxidative effluents. These effluents are produced by absorption or scrubbing processes used in treatment of gas streams (Boczka et al., 2016; Hariz et al., 2013; Sipma et al., 2004). To the best of our knowledge, no studies were made in such specific field of research. This research is focused on comparison of results for alkaline model WW with previous study (Boczka et al., 2017). The specific treatment methods that were studied in the present work were  $\text{O}_3$ ,  $\text{H}_2\text{O}_2$ ,  $\text{O}_3/\text{H}_2\text{O}_2$ , PS and PMS



processes. The effect of the dose of oxidant and the temperature are parameters under study.

## **2. Experimental**

### ***2.1 Materials***

Hydrogen peroxide (30%), sodium persulfate ( $\text{Na}_2\text{S}_2\text{O}_8$ ), potassium peroxymonosulfate ( $\text{KHSO}_5$ ) and sodium hydroxide were purchased from POCH (Poland). VOCs such as toluene, 2-ethyl-1-hexanol, phenol, were purchased from POCH (Poland), benzene, o-xylene, ethylbenzene, nitrobenzene, 2-nitrophenol, 2-nitrotoluene from Merck (Poland), 2-ethylthiophene, dibutyl sulfide, di-tert-butyl disulfide, 2,6-dimethylphenol, 4-methylbenzaldehyde and naphthalene from Sigma Aldrich (Poland) and 4-ethylphenol was purchased from Acros organics (a POCH product).

### ***2.2 Apparatus***

To conduct the experiments, an acid resistant steel closed cylindrical reactor was used, which can treat up to  $15 \text{ dm}^3$  of effluent. The details about the reactor are fully described in our previous work (Boczkaj et al., 2017). A semi-batch mode was used where the oxidant was added in a continuous mode during whole time of treatment. The model WW was pumped into the reactor by Euralca, model UGD 100/120-03, Italy membrane (PTFE) pump.  $\text{H}_2\text{O}_2$ ,  $\text{KHSO}_5$  and  $\text{Na}_2\text{S}_2\text{O}_8$  solutions were fed to the reactor using a Hitachi LaChrom HPLC Pump model L-7110. Ozone was fed by a Tytan 32 Ozone generator that is able to produce up to  $70 \text{ mg O}_3/\text{L}$  of oxygen. Dried air was used to produce ozone.

VOCs identification and quantification was performed by gas chromatography-mass spectrometry. The detailed description of the methods is described in our previous



paper (Boczka et al., 2016). COD determination was done using a HACH COD reactor and a HACH DR/2010 spectrophotometer.

### **2.3 Procedure**

#### **2.3.1. Model WW**

In order to simulate caustic effluents containing several VOCs, usually present in petroleum & refinery effluents, a model WW was prepared with the VOCs listed in section 2.1 with a concentration around  $10 \pm 2$  mg/L. The model WW has an initial pH of 10.5 and a measured COD between 390-490 mg O<sub>2</sub>/L.

#### **2.3.2. Effluent treatment**

To conduct all experiments performed, the model WW was prepared as followed; Firstly, 5 dm<sup>3</sup> of deionized water at a pH of 10.5 (the pH of the deionized water was corrected with 0.1 M NaOH) was pumped to the reactor and heated until the desired temperature. Afterwards a known volume of primary solution was added by the special injection port, present in the reactor using a 2 mL gas tight syringe. The final concentration of each compound in the model WW was  $10 \pm 2$  ppm. The initial pH was 10.5 in all procedures and no pH adjustment was performed during the treatment time. The volume of model WW treated was 5 dm<sup>3</sup>. The stirring was established at 200 rotations per minute (rpm). Regarding the oxidants used (H<sub>2</sub>O<sub>2</sub>, Na<sub>2</sub>S<sub>2</sub>O<sub>8</sub>, KHSO<sub>5</sub> and Ozone), their dose and treatment time are presented in Table 1. The pH of collected samples was measured by non-bleeding pH strips.

#### **2.3.3. Process control**

Every sample was taken with the purpose of analyzing the volatile organic compounds concentration, COD, and pH. COD was measured using the Polish standard test method PN-ISO 15705:2005, based on the dichromate method by HACH.

Regarding the VOCs monitoring, the sample preparation was done by dispersive liquid-liquid micro-extraction (DLLME) and analyzed by gas chromatography-mass spectrometry (GC-MS). Details of the procedure were fully described elsewhere (Boczkaj et al., 2016).

### 3. Results and discussion

The degradation efficiency of several VOCs in the basic pH water matrix was studied using H-AOPs (i.e., O<sub>3</sub>, H<sub>2</sub>O<sub>2</sub> and O<sub>3</sub>/H<sub>2</sub>O<sub>2</sub>) and S-AOPs (i.e., Na<sub>2</sub>S<sub>2</sub>O<sub>8</sub> and KHSO<sub>5</sub>). Comparison between H-AOPs and S-AOPs was possible in terms of VOCs degradation. The temperature and dose of oxidant were the parameters studied regarding the effectiveness of VOCs degradation.

#### 3.1. Degradation efficiency of H-AOPs

The degradation of VOCs by H-AOPs under different studied conditions has been shown in Figures 1S to 5S of supporting information (SI). To investigate the relative susceptibility of VOCs and the time required for their complete removal, the obtained results were carefully interpreted in detail.

Several VOCs such as VNCs, naphthalene and 4-methylbenzaldehyde were found to be persistent to sole-H<sub>2</sub>O<sub>2</sub> process (Figure 1S and Table 2). Their degradation starts after 120 min of treatment time and after benzene, toluene, ethylbenzene and o-xylene (BTEX) and phenol were degraded above 50%. Interestingly, 2-nitrophenol and 2-ethyltiophene revealed to be the by-products of other VOCs compounds as seen from their increasing concentration with treatment time. An interesting behavior was observed – when the concentration of toluene and benzene decreased, a corresponding increase in the concentration of 2-nitrophenol and 2-ethyltiophene was noted. There is evidence that 2-nitrophenol can be formed from phenol rings by reaction with nitrite

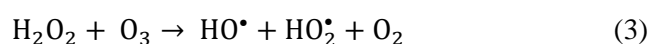
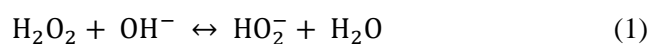


ions (Patnaik and Khoury, 2004). The Figure 1S and Table 2 results indicate that phenol degradation enables this pathway of 2-nitrophenol formation from phenolic compounds. In addition, it is proved that nitrite ions can be formed from  $N_2$  in the presence of  $H_2O_2$ . Even though this reaction occurs at a very low efficiency, only small amount of nitrite is needed to trigger the reaction (Gekhman et al., 2003; Vione et al., 2001) and in this study there is an excess of  $N_2$  which enables production of the nitrite ions. Furthermore, phenol can also be produced as an oxidation by-product of compounds containing benzene ring (Berndt and Böge, 2006), which can enhance the formation of 2-nitrophenol. A possible explanation for 2-ethylthiophene formation can be related with the oxidation and cyclization of sulfides and disulfides. These groups of compounds can be oxidized to sulfoxides by oxidation (Sato et al., 2001). The sulfoxides can produce thiophenes afterwards. Previous studies showed the cyclization of sulfoxides to thiophenes (Brown and Espenson, 1996; Wright et al., 1992). Furthermore, other VSCs such as di-tert-butyl disulfide and dibutyl sulfide were degraded fast after 15 min of treatment. Similar results were obtained in the degradation of dibutyl sulfide solely in a water matrix by  $H_2O_2$  at pH 12 but with a much higher dose of  $H_2O_2$  applied (Popiel et al., 2009). After 120 min of treatment, most of the O-VOCs reached higher degradation efficiencies.

It is clear that sole use of  $H_2O_2$ , was less efficient comparing with  $O_3$ , and  $O_3/H_2O_2$  for all VOCs studied. Fortunately, higher  $H_2O_2$  dose had a positive effect on the degradation of VOCs that were more persistent to degradation. This can be related with the increase of the oxidant amount in the water matrix or even the local decrease of pH in the bulk of effluents during treatment which favors the efficiency of  $H_2O_2$ . The decrease of the pH during treatment is related with the addition of  $H_2O_2$  and with the degradation of the pollutants present in the water matrix to more acidic compounds like



carboxylic acids. Under basic conditions, H<sub>2</sub>O<sub>2</sub> reacts with HO<sup>-</sup> to form perhydroxyl ions (HO<sub>2</sub><sup>-</sup>) (reaction 1) which has significantly lower oxidation potential than HO<sup>•</sup> (Spalek et al., 1982). H<sub>2</sub>O<sub>2</sub> can only produce HO<sup>•</sup> by the activation of ultraviolet light (reaction 2) or in combination with ozone (reaction 3) or even by a catalyst like iron, the so called Fenton related AOPs (Shah et al., 2018b) .



Furthermore, the oxidation potential of H<sub>2</sub>O<sub>2</sub> is significantly lower than that of O<sub>3</sub> which also influences the overall efficiency of the treatment. These reasons can explain the relatively low effectiveness of H<sub>2</sub>O<sub>2</sub> at these conditions. Both O<sub>3</sub> and O<sub>3</sub>/H<sub>2</sub>O<sub>2</sub> processes have high effectiveness at the parameters studied obtaining around 100% degradation of all VOCs studied. The generation of HO<sup>•</sup> using O<sub>3</sub> at basic pH may explain such increase in the overall degradation efficiency of VOCs.

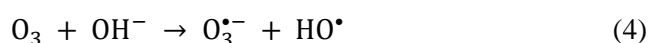
Figure 2S presents the degradation of the VOCs in the presence of O<sub>3</sub> with a dose of 35 g. It clearly shows that BTEX, phenol and VSCs reach almost complete degradation in the first 15 min of treatment. 2-nitrophenol was completely degraded in the first 30 min of oxidation. Afterwards, the oxidant molecules reacted mainly with di-tert-butyl disulfide, naphthalene and phenolic compounds until their almost complete oxidation at 120 min of treatment. 4-methylbenzaldehyde was degraded 66% in the first 15 min of treatment but remains constant until 120 min and afterwards is degraded completely at 181 min of treatment. Interestingly, 2,6-dimethylphenol and 2-nitrophenol which were found to be completely degraded at 120 min of treatment reappeared at 181 min with an increase of 15 and 8%, respectively. The reappearance of 2-nitrophenol could possibly be linked with the degradation of the nitrobenzene by HO<sup>•</sup> from 80 to 94% from 120 min to the end of the treatment. The “attack” of HO<sup>•</sup> on the benzene ring



can lead to the addition of the HO group to the ring and hence, to the formation of 2-nitrophenol from nitrobenzene. Another hypothesis can be related with other compounds (formed during the treatment of this model effluents, not detected by the method used) that include 2-nitrophenol in their degradation pathway. With respect to the formation of 2,6-dimethylphenol, the oxidation of 4-methylbenzaldehyde, nitrobenzene or 2-nitrotoluene cannot explain its increase, since their degradation, according to their chemical structure, is not favoring a formation of 2,6-dimethylphenol. A possible hypothesis is that some compounds, not detected by the methods used, can actually include this compound in their degradation pathways. Figure 3S describes the VOCs degradation using O<sub>3</sub> with a dose of 70 g. Once again, the BTEX, phenol, 2-ethylthiophene and 2-nitrophenol were degraded with effectiveness at 15 min of treatment. The most interesting behavior in this process was the degradation of 4-methylbenzaldehyde and 2,6-dimethylphenol. These compounds only started to degrade significantly after 120 min of treatment, when all other compounds were oxidized more than 80%. One possible explanation for the persistency of the oxidation of 4-methylbenzaldehyde can be related with the fact that this compound can be a by-product of nitrobenzene and phenolic compounds (Sun et al., 1995; Zheng et al., 1993). VNCs had a slow degradation rate after 30 min of treatment. Similar results were obtained in a recent work by Gałol et al. (2018) with similar compounds under basic pH using same dose of O<sub>3</sub> aided by hydrodynamic or acoustic cavitation. Gałol et al. (2018) found slightly higher degradation efficiency for 4-ethylphenol and di-tert-butyl disulfide and lower for phenol. In the present case, the process is simpler and less expensive than ultrasonic technology and achieved similar results, making it more effective. Overall, VNCs and 4-methylbenzaldehyde were more persistent to degradation with O<sub>3</sub>. The HO• are more likely to attack compounds with high electron density such as double



bonds and aromatic rings (Chen et al., 2014). Thus, the degradation efficiency of aromatic compounds is higher than non-aromatic or simple bond compounds. In addition, electron donor groups such as NH<sub>2</sub> and OCH<sub>3</sub>, could accelerate the degradation rate of aromatic compounds (Chen et al., 2014), which can explain the higher degradation efficiency of BTEX and phenolic compounds. Furthermore, sulfur atom increases the reaction rate with HO<sup>•</sup> due to the electron donating properties (Kwok and Atkinson, 1995). This is proved in this work where the VSCs are degraded with the highest efficiency. However, the presence of NO<sub>x</sub> groups on aromatic and linear compounds, decreases the degradation efficiency of the VNCs in general (Chen et al., 2014). The higher degradation efficiency of these compounds by O<sub>3</sub> comparing with H<sub>2</sub>O<sub>2</sub> can be related with the reaction mechanism. Ozone is able to transform the organic compounds due to its high oxidation potential (E<sup>0</sup> = 2.07 V) (Chandrasekara Pillai et al., 2009; Esplugas et al., 2002; Kusic et al., 2006). When present in alkaline medium, O<sub>3</sub> directly reacts with HO<sup>-</sup> to generate HO<sup>•</sup> (reaction 4) (Alaton et al., 2002; Poyatos et al., 2010; Katsoyiannis et al., 2011).



Thus, a higher amount of free reactive species is available to degrade the VOCs, namely HO<sup>•</sup> (more reactive species than H<sub>2</sub>O<sub>2</sub> and O<sub>3</sub>). Figures 2S and 3S reveal that increase of the dose significantly affected the rate of VOCs degradation, namely 4-methylbenzaldehyde and 2,6-dimethylphenol. These two compounds had lower degradation rate in the first 120 min of treatment with a higher applied dose of O<sub>3</sub>. Moreover, these compounds, especially 4-methylbenzaldehyde can be a by-product of oxidation of phenolic compounds. By comparing with H<sub>2</sub>O<sub>2</sub>, a lower dose of O<sub>3</sub> was needed to achieve similar VOCs degradation efficiency. This can be related with the oxidation potential of O<sub>3</sub> and with the presence of HO<sup>•</sup> which can degrade the VOCs



faster. These results are similar to the use of O<sub>3</sub> in the treatment of phenol solely in a water matrix at basic pH (Esplugas et al., 2002).

O<sub>3</sub>/H<sub>2</sub>O<sub>2</sub> process was found to be more effective than O<sub>3</sub> and H<sub>2</sub>O<sub>2</sub> (Figures 4S and 5S). The combination of O<sub>3</sub> and H<sub>2</sub>O<sub>2</sub> allow indirect and direct oxidation of organic compounds (Alaton et al., 2002; Ameta et al., 2013). H<sub>2</sub>O<sub>2</sub> will promote the degradation of O<sub>3</sub> by electron transfer or alternatively the O<sub>3</sub> will activate the H<sub>2</sub>O<sub>2</sub> which generates HO• and HO<sub>2</sub>• (reaction 5) (Alsheyab and Muñoz, 2006; Safarzadeh-Amiri, 2001; Wu et al., 2007).

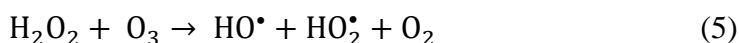


Figure 4S describes the VOCs degradation using O<sub>3</sub>/H<sub>2</sub>O<sub>2</sub> with a dose of 98 g (O<sub>3</sub> = 48.5 g and H<sub>2</sub>O<sub>2</sub> = 49.5 g). All VOCs were degraded very quickly in just only 15 min of treatment except 2-nitrophenol which took 60 min for its complete removal. Once again, BTEX, phenol, 2-ethylthiophene and dibutyl sulfide were the first compounds to be degraded after 15 min of treatment. Other studies also reported the effective degradation of dibutyl sulfide and phenol by O<sub>3</sub>/H<sub>2</sub>O<sub>2</sub> at basic pH in a one compound model WW (Esplugas et al., 2002; Popiel et al., 2009). When O<sub>3</sub>/H<sub>2</sub>O<sub>2</sub> dose was increased from 98 (O<sub>3</sub> 48.5 g and H<sub>2</sub>O<sub>2</sub> 49.5 g) to 189 g (O<sub>3</sub> 61.5 g and H<sub>2</sub>O<sub>2</sub> 127.5 g) at 40 °C, the degradation efficiency for all the studied compounds increased significantly as revealed from comparing the residues concentration at 15 min of treatment in Figures 4S and 5S. VNCs and 4-methylbenzyldehyde were found to be relatively more persistent to degradation in the peroxone processes.

Figure 1 depicts an insight into the relative susceptibility of the tested VOCs towards O<sub>3</sub>, H<sub>2</sub>O<sub>2</sub> and O<sub>3</sub>/H<sub>2</sub>O<sub>2</sub> processes and a better comparison of the studied oxidation processes. It can be seen that VNCs were more persistent to degradation in all processes studied due to the presence of the NO<sub>2</sub> group which decreases the degradation



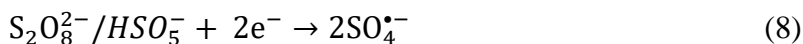
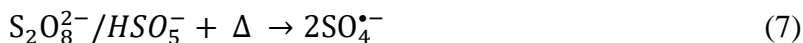
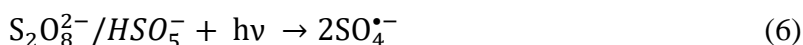
efficiency. This difference was more significant and relevant in the  $\text{H}_2\text{O}_2$  processes. The BTEX, phenol and VSCs were the fastest degraded compounds by these technologies. 2-nitrophenol was easy to degrade only in the  $\text{O}_3$  related processes. 4-methylbenzaldehyde, 2-nitrotoluene and nitrobenzene were compounds that reveal persistency to degradation and are the last compounds to degrade by all the studied technologies. In  $\text{O}_3/\text{H}_2\text{O}_2$  process, complete degradation of all VOCs was reached at 60 min of treatment. Thus, it was possible to stop the process at that time, decreasing the dose of oxidant needed from 189 to 36 g (Figure 5S) and from 98 to 24 g at 40 °C (Figure 4S), i.e., 4 and 5.2 times decrease in oxidant dose, respectively. In addition, they are lower than  $\text{O}_3$  and  $\text{H}_2\text{O}_2$  processes, making it more effective and less costly in terms of chemicals. Comparable results were obtained in a similar work, using the same compounds at basic pH, but using peroxone alone and aided with hydrodynamic or acoustic cavitation (Gałol et al., 2018). At 30 min of oxidation, all compounds with one exception (in this work 2-nitrophenol and in ultrasonic technology nitrobenzene) were completely degraded. In summary, the  $\text{O}_3/\text{H}_2\text{O}_2$  process is more effective to degrade VOCs of effluent at basic pH with a dose of 23.5 g ( $\text{H}_2\text{O}_2 = 11.9$  g and  $\text{O}_3 = 11.6$  g) at 40 °C. These processes and its operational conditions are able to treat the VOCs in a relatively short time, degrading the most problematic compounds to treat in these type of effluents, making the biological treatment stage easier – with lower pollution load and less toxic to activated sludge compounds.

### 3.2. *S-AOPs: performance of PS and PMS technologies*

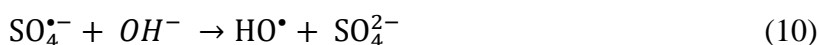
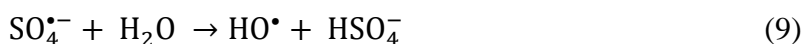
Persulfate (PS) and peroxydisulfate (PMS) are popular alternative to the classic oxidants used in the advanced oxidation technologies. Both PS and PMS have the potential to generate  $\text{SO}_4^{\bullet-}$  through their activation by UV light (reaction 6), heat (reaction 7) or a catalyst (Sayed et al., 2018).  $\text{SO}_4^{\bullet-}$  have an oxidation potential ( $E^\circ$ ) of



2.6 V (Devi et al., 2016; Ghauch et al., 2012; Liu et al., 2013; Waclawek et al., 2017), making them highly reactive species.



The persulfate anion ( $S_2O_8^{2-}$ ) and peroxymonosulfate anion ( $HSO_5^-$ ) are strong oxidants, with  $E^0$  of 2.01 and 1.85 V, respectively. These can be used for degradation of wide range of organic contaminants (Liang et al., 2011; Long et al., 2014; Oh et al., 2011; Rehman et al., 2018; Shah et al., 2018a). Sulfate radicals in aqueous medium and at basic medium can generate  $HO^{\bullet}$  (reactions 9 and 10) (Boczkaj and Fernandes, 2017).



Alternatively, PS and PMS can be activated by the use of a base (e.g., NaOH) (reaction 11) (Furman et al., 2010; Qi et al., 2016).

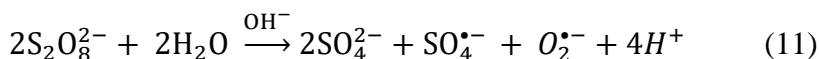


Figure 2 and Table 3 reveal that increasing the oxidant dose and temperature in PS and PMS processes significantly increase the degradation efficiency of the studied VOCs. The difference is more significant when the temperature was increased from 40 to 60 °C. The activation of  $S_2O_8^{2-}$  and  $HSO_5^-$  to  $SO_4^{\bullet-}$  by heat is the main factor for such increase. The increase of the oxidant dose from 218 to 436 g while keeping the temperature constant led to a small increase in the VOCs degradation. Comparing both processes under the same conditions, PS revealed to be more effective than PMS technology, due to the higher oxidation potential of PS than PMS. Comparing with  $H_2O_2$ , S-AOPs degraded the VOCs with higher effectiveness. On the other hand, by comparing with  $O_3$  related processes, S-AOPs achieved lower degradation efficiencies.

PS and PMS processes were also studied for the degradation profile of each compound during oxidation time. For PS process at 40 °C with a dose of 436 g, Figure 6S reveals that, as demonstrated in classic AOPs, VNCs, namely 2-nitrotoluene and nitrobenzene were persistent to degradation. 2-nitrotoluene reached 20% degradation after 30 min and it remains at the same level until the end of the treatment. Nitrobenzene achieved 45% of degradation after 30 min and remains the same until 120 min of treatment, only after this time it was degraded further up to 67% of degradation. VSCs and 2-nitrophenol were degraded faster after 30 min of treatment. On the opposite trend of the H-AOP, BTEX and phenol started to be effectively degraded at the moment when the VSCs and the other O-VOCs were almost totally degraded. When the oxidant dose was kept constant and the temperature increased from 40 to 60 °C, positive effect on removal efficiency was observed (Figure 7S). 2-nitrotoluene and nitrobenzene were degraded efficiently, especially after 60 min of treatment. Again, BTEX started to degrade when ca. 95% degradation was achieved for VSCs and other O-VOCs. When the temperature was kept constant at 60 °C and the oxidant dose decreased a half to 218 g, the degradation rate was similar for VSCs and O-VOCs, with differences only in three compounds (Figure 8S). Figure 8S shows that 4-methylbenzaldehyde had a slower degradation rate comparing with the Figure 7S because of two possible reasons. First, it indicates that the lower dose of oxidant still performs effective degradation for the most VOCs with exemption of compounds more persistent to degradation by this type of processes. Second, such behavior can also be related to the fact that 4-methylbenzaldehyde can be a by-product of oxidation of phenolic compounds such as 4-ethylphenol or nitrophenols (Sun et al., 1995; Zheng et al., 1993). Lower dose of oxidant could possibly be effective in degrading the target compounds but the degradation of produced by-products could be slower due to the lower concentration of





reactive radicals. In the cases of 2-nitrotoluene and nitrobenzene, they were removed only 65 and 76%, respectively, and their degradation occurred mainly in the first 60 min. During further treatment, the degradation rate started to be lowering until the end of the treatment. The same phenomenon was observed at 40 °C (Figure 6S) with the same compounds but at lower degradation (21 and 66% respectively). This effect can probably be related to radical scavenging by the by-products of oxidation of the other VOCs. In addition, the cations present in the water matrix and residual sulfate formation, due to the salt addition (PS and PMS) can also affect the oxidation by scavenging the radical species (Boczkaj and Fernandes, 2017; Huang et al., 2005). This can be a negative outcome of the usage of S-AOPs.

Figures 9S and 10S report the degradation profile of the VOCs for the PMS processes at a fixed dose of 114 g at 40 and 60 °C, respectively. 2-nitrotoluene and nitrobenzene were degraded below 10%, proving to be very persistent to oxidation by PMS process. VSCs were once more the easiest to degrade, with effective degradation after 60 min of treatment. The only exception was 2-ethylthiophene in the process at 40 °C, with only 10% of degradation. O-VOCs had a small increase in their degradation when the temperature was increased from 40 to 60 °C. When the oxidant was decreased from 114 to 70 g while keeping the temperature constant at 60°C, some positive results were observed (Figure 11S). VSCs and 2-nitrophenol achieved almost complete degradation after 15 min of treatment. After 15 min of treatment, all other compounds started to be significantly degraded. The most interesting behavior was the degradation of 2-nitrotoluene and nitrobenzene up to 80% after 120 treatment. One reason for such significant difference can be related with the decrease of the PMS concentration. Too high amount of PMS present in the water matrix can have a detrimental effect on its own activation to sulfate radicals or in the yield of the radicals formation. PMS can



react with himself or even with the  $\text{SO}_4^{\bullet-}$  producing sulfate ions or less reactive radical species. Thus, decreasing the amount of PMS from 114 to 70 g was beneficial to the overall degradation of VOCs.

The activation of PS and PMS by heat had a positive effect in the VOCs degradation which could help in decreasing the amount of oxidant used for the same degree of VOCs degradation. Comparing PS and PMS technologies, PS revealed to be more effective in VOCs degradation than PMS, probably due to a higher efficiency of the activation of PS than PMS. In addition, the oxidation potential of PS is higher than PMS which could also influence the results.

Furthermore, the activation of PMS by heat had a positive effect making possible to decrease the amount of oxidant used by half and at the same time achieving higher removal efficiencies. Overall, these results proved that VOCs were the first to degrade and achieved total degradation in both PS and PMS processes. VNCs were more persistent to degradation by both technologies. In case of the specific compounds, VOCs and 2-nitrophenol were the compounds to degrade first and 2-nitrotoluene and nitrobenzene were more persistent and needed more time to reach high degradation values. PS process with a dose of 436 g at 60 °C and PMS process with a dose of 70 g at the same temperature reached higher percentage of degradation of the VOCs, with 98.6% and 95.6% of total-VOCs degradation, respectively. Taking this data into account and the dose used of each oxidant, it can be concluded that in fact PMS process needs less amount of oxidant, being more effective than PS process.

Nevertheless, to decide which process is more effective, a study of the by-products of oxidation was performed to check if any by-products of oxidation are present and if they can be toxic and more harmful to biological approaches than the initial VOCs.



### 3.3. *Identification of by-products*

Since the ultimate goal of water treatment technologies is to reduce water toxicity, it is crucial to identify the by-products of the target VOCs to understand if there is a risk of harmful and persistent by-products formation. In addition, it can be helpful to understand some pathways of degradation of the compounds when present in multiple artificial WW. Keeping this desirable goal in mind, the final sample from each process studied was submitted to additional GC-MS analysis in SCAN mode to identify and quantify all VOCs present in the end of the process. Figures 12S to 16S show the chromatograms of the initial and final sample of the H-AOPs and Figures 17S to 24S are the chromatograms from the S-AOPs. The peaks marked as IS, represent the internal standards. In respect to the H<sub>2</sub>O<sub>2</sub> process, Figure 12S reveals the absence of any by-products formed during the treatment. Only the 2-nitrophenol peak had an increase after treatment as already discussed. Figure 13S shows the chromatogram of the O<sub>3</sub> process with a dose of 35 g. It is possible to verify that the compounds studied were almost completely degraded with exception of dibutyl sulfide and 4-methylbenzaldehyde whose degradation was insignificant. No harmful VOCs were detected, suggesting a good and efficient VOCs treatment option. The chromatogram of the O<sub>3</sub> process with a dose of 70 g is presented as Figure 14S. This Figure revealed an effective degradation of all compounds in the model WW due to a “clean” chromatogram of the sample after treatment. Regarding the O<sub>3</sub>/H<sub>2</sub>O<sub>2</sub> process, Figures 15S and 16S show almost completely clean chromatograms except the presence of dibutyl sulfide peak, which was under the limit of detection (LOD). These processes revealed to be very effective due to the lack of harmful by-products formation. Since no harmful or non-biodegradable by-products were detected, the obtained results proved that the risk of emission of compounds is eliminated in one single and simple stage. It is proved that O<sub>3</sub>/H<sub>2</sub>O<sub>2</sub>

process could effectively degrade the VOCs with no toxic by-products formation. As a result, O<sub>3</sub>/H<sub>2</sub>O<sub>2</sub> process with a dose of 24 g at 40 °C continues to be the best choice.

Regarding the S-AOPs, only one by-product was identified after treatments. It is acetophenone and it is identified in all processes with exception of PS at 60 °C with a dose of 436 g and in PMS process at 60 °C with a dose of 114 g. Nevertheless, the peak is very small. The acetophenone can be produced from the oxidation of ethylbenzene or 4-ethylphenol. The formation of acetophenone from ethylbenzene oxidation has already been reported (Ghiaci et al., 2010). The only big peak on the chromatograms represents the IS added to the samples prior the extraction step and the minor peaks represent the compounds that were not below LOD, like nitrobenzene, 2-nitrotoluene, 4-methylbenzaldehyde, 2-ethyl-1-hexanol and ethylbenzene. With this data, we can conclude that PMS process with a dose of 70 g at 60 °C is a better approach, with no harmful and toxic by-products, having a clean chromatogram after treatment, than PS process with a dose of 436 g at 60 °C. The significant difference between doses of oxidants used led to the conclusion that the PMS process is the most suitable approach using S-AOPs when treating VOCs.

### **3.4. Comparison between classic H-AOPs and S-AOPs**

The trend is equal in H-AOPs and S-AOPs in terms of total VNCs, VSCs and O-VOCs degradation. The VSCs were the easiest to be degraded whereas VNCs were the most persistent. Regarding the total VOCs degradation, the H<sub>2</sub>O<sub>2</sub> technology was the poorest as expected due to the fact that alone H<sub>2</sub>O<sub>2</sub> does not produce high reactive radicals under basic pH conditions. PS and PMS revealed to be more effective than H<sub>2</sub>O<sub>2</sub>. PS and PMS are not only more stable in aqueous solutions but also have weaker O-O bonds than H<sub>2</sub>O<sub>2</sub> which make them easier to dissociate and generate reactive species (Ike et al., 2018). Comparing PS and PMS with O<sub>3</sub> and O<sub>3</sub>/H<sub>2</sub>O<sub>2</sub>, O<sub>3</sub> related

processes were more effective and achieved total degradation of all compounds. In terms of specific compounds, HO<sup>•</sup> are able to react first with BTEX, phenol and VSCs compounds and are less effective in the degradation of 2-nitrotoluene, nitrobenzene and 4-methylbenzaldehyde in accordance with reactivity effect of the electrons donating and withdrawing groups, respectively. As far as SO<sub>4</sub><sup>•-</sup> is concerned, it reacts first with the other O-VOCs, like non-aromatics, 2-nitrophenol and VSCs and afterwards with phenol and BTEX. Like HO<sup>•</sup>, SO<sub>4</sub><sup>•-</sup> has lower reactivity with 2-nitrotoluene, nitrobenzene and 4-methylbenzaldehyde. The degradation of all VOCs was slower with S-AOPs. The reaction mechanism can explain the different reactivity of HO<sup>•</sup> and SO<sub>4</sub><sup>•-</sup> towards studied VOCs. HO<sup>•</sup> reacts mainly by addition to the multiple C-C, C-N and C-S bonds and by H-abstraction, even though it can react by electron transfer mechanism (von Sonntag, 2005). HO<sup>•</sup> prefers to react by addition to the aromatic rings. In case of SO<sub>4</sub><sup>•-</sup>, it rather prefers to react by electron transfer and its H-abstraction reaction is much slower than that of HO<sup>•</sup> (Neta et al., 1988). Comparing the best processes of H-AOPs and S-AOPs, it is possible to check several disadvantages of PMS process comparing with O<sub>3</sub>/H<sub>2</sub>O<sub>2</sub>. Firstly, PMS process takes more time to reach similar degradation than O<sub>3</sub>/H<sub>2</sub>O<sub>2</sub>. Secondly, not all VOCs were degraded by PMS process as did by O<sub>3</sub>/H<sub>2</sub>O<sub>2</sub>. Thirdly, the temperature needed for the PMS and PS process requires extra heating of the effluents making the process more expensive. Finally, the residual sulfate generated from the oxidation can have a negative impact on biological technologies, but this hypothesis needs to be proved properly. Thus, S-AOPs are less effective and suitable to be a good option for treatment of such type of effluents. Summing up, O<sub>3</sub>/H<sub>2</sub>O<sub>2</sub> is actually the best choice to perform an effective removal of all VOCs studied. The absence of VOCs in treated effluent is an important factor in relation to biological stage



of treatment. Biological processes are conducted in open air reservoirs and thus could cause the emission of VOCs, present in the effluent, into the atmosphere.

### 3.5. *Economic evaluation*

Selection of a proper treatment technology for specific type of real effluents is not based only on the effectiveness of the technology but also depends on its cost, when taking the decision to apply in the real case scenario. To check either these technologies are viable to implement in a real case scenario, a basic economic evaluation was performed. A similar methodology was followed as performed by Gagol and co-workers (Gagol et al., 2018). The prices of the oxidants used in this work were assumed to perform the calculations.  $\text{H}_2\text{O}_2$  had a cost of 8.2 American dollars per liter (\$/L),  $\text{Na}_2\text{S}_2\text{O}_8$  was purchased by 40.74 \$/L and  $\text{KHSO}_5$  by 56.58 \$/L. In Poland, the price of electricity to industrial customers is around 0.11 \$/kWh (3600 kJ). Furthermore, the power of the ozone generator and pump, responsible to introduce the oxidants into the reactor during treatment time was also included in the cost calculation. Ozone generator and oxidant pump have working powers of 450 and 80 W, respectively. To determine the cost of treatment, it was assumed that the treatment time used in this work was enough to obtain an effective degradation, i.e., higher than 95% of the studied VOCs. Table 4 represents the cost of each technology studied. The cost of treatment was assumed to be a combined value of the chemical and energy costs. The cost calculations clearly show that H-AOPs are much cheaper than S-AOPs, mainly due to the price of oxidants. The difference is around two orders of magnitude giving a clear idea that S-AOPs are not economically viable to implement in an industrial facility. Among the H-AOPs, peroxone revealed to be the cheapest, comparing to  $\text{H}_2\text{O}_2$  and  $\text{O}_3$ . Also, it is interesting to see that  $\text{O}_3$  process is slightly cheaper than  $\text{H}_2\text{O}_2$  treatment. The treatment cost obtained in this work for the H-AOPs are lower than the ones obtained in a similar



study at the same operational conditions (Gagol et al., 2018). Taking into account that the cost evaluation was performed using large laboratory scale data, a cost of treatment per liter between 3 and 6 cents of American dollars is cheap and viable. To conclude this section, implementation of such technologies is feasible for real WW effluents due to their cheapness (3 to 6 cents of American dollars are needed for treatment of 1 L effluent) and simplicity (only a stirred tank and an ozone generator are needed).

#### 4. Conclusions

The study of oxidation of several VOCs in simulated caustic effluents from bitumen production using  $O_3$ ,  $O_3/H_2O_2$ ,  $H_2O_2$ ,  $Na_2S_2O_8$  and  $KHSO_5$  was performed with attempt for effective VOCs degradation, eliminating the most problematic compounds from this type of effluents. This is a huge step to reach a good quality of treated effluent for possible water re-utilization and to improve the aspect of “cleaner technologies” of bitumen production. Comparison between H- and S-AOPs, i.e., the behavior of hydroxyl and sulfate radicals in degradation of several VOCs was studied.

The peroxone ( $O_3/H_2O_2$ ) process with a dose of 23.5 g ( $H_2O_2$ : 11.9 g and  $O_3$ :11.6 g) at 40 °C was the most efficient technology to degrade the model WW. S-AOPs were more efficient than  $H_2O_2$  especially at 60 °C. Further increase of temperature was not studied due to the impractical value of such conditions related to energy costs of effluent heating. VSCs achieved higher degradation in a shortest treatment time and VNCs were the most persistent compounds to degradation in all technologies studied. The BTEX degradation time and efficiency differs in H-AOPs and S-AOPs. This can be related with a different oxidation mechanism of  $HO^\bullet$  and  $SO_4^{\bullet-}$  ( $HO^\bullet$  reacts mainly via addition and  $SO_4^{\bullet-}$  via electron transfer).

The study of by-products revealed that no toxic, complex and non-biodegradable by-products were identified after treatment. The cost evaluation revealed that H-AOPs are two orders of magnitude cheaper than S-AOPs. Peroxone revealed to be the cheaper technology with a cost of treatment between 0.03 and 0.04 \$/L of model effluent treated. Classical H-AOPs can be described as cheap and easy technologies to implement for VOCs degradation. The compounds studied in this research are also present in different types of industrial, especially refinery origin, effluents. Thus the obtained data are also useful to other branches of wastewater treatment.

### Acknowledgments

The authors gratefully acknowledge the financial support from the National Science Center, Warsaw, Poland – decision no. DEC-2013/09/D/ST8/03973 and UMO-2017/25/B/ST8/01364. The authors would like to thank also the Lotos Asphalt, Ltd. (Grupa Lotos) for their cooperation on this project.

### References

- Alaton, I.A., Balcioglu, I.A., Bahnemann, D.W., 2002. Advanced oxidation of a reactive dyebath effluent: Comparison of O<sub>3</sub>, H<sub>2</sub>O<sub>2</sub>/UV-C and TiO<sub>2</sub>/UV-A processes. *Water Res.* 36, 1143–1154. [https://doi.org/10.1016/S0043-1354\(01\)00335-9](https://doi.org/10.1016/S0043-1354(01)00335-9)
- Ali, F., Khan, J.A., Shah, N.S., Sayed, M., Khan, H.M., 2018. Carbamazepine degradation by UV and UV-assisted AOPs: Kinetics, mechanism and toxicity investigations. *Process Saf. Environ. Prot.* 117, 307-314. <https://doi.org/10.1016/j.psep.2018.05.004>
- Alsheyab, M.A., Muñoz, A.H., 2006. Reducing the formation of trihalomethanes (THMs) by ozone combined with hydrogen peroxide (H<sub>2</sub>O<sub>2</sub>/O<sub>3</sub>). *Desalination* 194, 121–126. <https://doi.org/10.1016/j.desal.2005.10.028>
- Ameta R, Kumar A, Punjabi PB, A.S., 2013. Advanced oxidation Processes: Basics and Principles, in: Rao DG, Senthilkumar R, Anthony Byrne J, F.S. (Ed.), *Wastewater Treatment: Advanced Processes and Technologies*. CRC Press and IWA publishing, USA, pp. 61–107. <https://doi.org/10.1007/s13398-014-0173-7.2>
- Autelitano, F., Giuliani, F., 2018. Analytical assessment of asphalt odor patterns in hot mix asphalt production. *J. Clean. Prod.* 172, 1212–1223.





<https://doi.org/10.1016/j.jclepro.2017.10.248>

- Bahri, M., Mahdavi, A., Mirzaei, A., Mansouri, A., Haghghat, F., 2018. Integrated oxidation process and biological treatment for highly concentrated petrochemical effluents: A review. *Chem. Eng. Process. - Process Intensif.* 125, 183–196. <https://doi.org/10.1016/j.cep.2018.02.002>
- Berndt, T., Böge, O., 2006. Formation of phenol and carbonyls from the atmospheric reaction of OH radicals with benzene. *Phys. Chem. Chem. Phys.* 8, 1205. <https://doi.org/10.1039/b514148f>
- Boczkaj, G., Fernandes, A., 2017. Wastewater treatment by means of Advanced Oxidation Processes at basic pH conditions: A review. *Chem. Eng. J.* 320, 608–633. <https://doi.org/10.1016/j.cej.2017.03.084>
- Boczkaj, G., Fernandes, A., Makoś, P., 2017. Study of Different Advanced Oxidation Processes for Wastewater Treatment from Petroleum Bitumen Production at Basic pH. *Ind. Eng. Chem. Res.* 56, 8806–8814. <https://doi.org/10.1021/acs.iecr.7b01507>
- Boczkaj, G., Kamiński, M., Przyjazny, A., 2010. Process Control and Investigation of Oxidation Kinetics of Postoxidative Effluents Using Gas Chromatography with Pulsed Flame Photometric Detection (GC-PFPD). *Ind Eng Chem Res* 49, 12654–12662.
- Boczkaj, G., Makoś, P., Przyjazny, A., 2016. Application of dispersive liquid-liquid microextraction and gas chromatography-mass spectrometry (DLLME-GC-MS) for the determination of oxygenated volatile organic compounds in effluents from the production of petroleum bitumen. *J. Sep. Sci.* 39, 2604–2615.
- Boczkaj, G., Przyjazny, A., Kamiński, M., 2014. New Procedures for Control of Industrial Effluents Treatment Processes. *Ind Eng Chem Res* 56, 1503–1514.
- Brown, K.N., Espenson, J.H., 1996. Stepwise Oxidation of Thiophene and Its Derivatives by Hydrogen Peroxide Catalyzed by Methyltrioxorhenium(VII). *Inorg. Chem.* 35, 7211–7216. <https://doi.org/10.1021/ic960607+>
- Chandrasekara Pillai, K., Kwon, T.O., Moon, I.S., 2009. Degradation of wastewater from terephthalic acid manufacturing process by ozonation catalyzed with Fe<sup>2+</sup>, H<sub>2</sub>O<sub>2</sub> and UV light: Direct versus indirect ozonation reactions. *Appl. Catal. B Environ.* 91, 319–328. <https://doi.org/10.1016/j.apcatb.2009.05.040>
- Chen, Z., Yu, X., Huang, X., Zhang, S., 2014. Prediction of reaction rate constants of hydroxyl radical with organic compounds. *J. Chil. Chem. Soc.* 59, 2252–2259. <https://doi.org/10.4067/S0717-97072014000100003>
- Cheng, H.-H., Hsieh, C.-C., 2013. Removal of Aromatic Volatile Organic Compounds in the Sequencing Batch Reactor of Petroleum Refinery Wastewater Treatment Plant. *CLEAN - Soil, Air, Water* 00, n/a-n/a. <https://doi.org/10.1002/clen.201100112>
- Devi, P., Das, U., Dalai, A.K., 2016. In-situ chemical oxidation: Principle and applications of peroxide and persulfate treatments in wastewater systems. *Sci. Total Environ.* <https://doi.org/10.1016/j.scitotenv.2016.07.032>
- Espugas, S., Giménez, J., Contreras, S., Pascual, E., Rodríguez, M., 2002. Comparison of different advanced oxidation processes for phenol degradation. *Water Res.* 36,

1034–1042. [https://doi.org/10.1016/S0043-1354\(01\)00301-3](https://doi.org/10.1016/S0043-1354(01)00301-3)

- Fernandes, A., Makos, P., Boczkaj, G., 2018. Treatment of bitumen post oxidative effluents by sulfate radicals based advanced oxidation processes ( S-AOPs ) under alkaline pH conditions. *J. Clean. Prod.* 195, 374–384.  
<https://doi.org/10.1016/j.jclepro.2018.05.207>
- Furman, O.S., Teel, A.L., Watts, R.J., 2010. Mechanism of base activation of persulfate. *Environ. Sci. Technol.* 44, 6423–6428. <https://doi.org/10.1021/es1013714>
- Gągol, M., Przyjazny, A., Boczkaj, G., 2018. Highly effective degradation of selected groups of organic compounds by cavitation based AOPs under basic pH conditions. *Ultrason. Sonochem.* 45, 257–266.  
<https://doi.org/10.1016/j.ultsonch.2018.03.013>
- Gekhman, A.E., Stolyarov, I.P., Shestakov, A.F., Shilov, A.E., Moiseev, I.I., 2003. Oxidation of molecular nitrogen with hydrogen peroxide \*. *Russ.Chem.Bull., Int.Ed* 52, 768–770.
- Ghanbari, F., Moradi, M., Moradi, M., 2016. Application of peroxymonosulfate and its activation methods for degradation of environmental organic pollutants : Review. *Chem. Eng. J.* <https://doi.org/10.1016/j.cej.2016.10.064>
- Ghauch, A., Tuqan, A.M., Kibbi, N., 2012. Methylene blue discoloration by heated persulfate in aqueous solution. *Chem. Eng. J.* 197, 483–492.  
<https://doi.org/10.1016/j.cej.2012.05.051>
- Ghiaci, M., Molaie, F., Sedaghat, M.E., Dorostkar, N., 2010. Metalloporphyrin covalently bound to silica. Preparation, characterization and catalytic activity in oxidation of ethyl benzene. *Catal. Commun.* 11, 694–699.  
<https://doi.org/10.1016/j.catcom.2010.01.023>
- Glaze, W.H., Kangt, J., 1989. Advanced Oxidation Processes . Test of a Kinetic Model for the Oxidation of Organic Compounds with Ozone and Hydrogen Peroxide in a Semibatch Reactor. *Ind. Eng. Chem. Res.* 28, 1580–1587.  
<https://doi.org/10.1021/ie00095a002>
- Goel, M., Hongqiang, H., Mujumdar, A.S., Ray, M.B., 2004. Sonochemical decomposition of volatile and non-volatile organic compounds - A comparative study. *Water Res.* 38, 4247–4261. <https://doi.org/10.1016/j.watres.2004.08.008>
- Hariz, I. Ben, Halleb, A., Adhoum, N., Monser, L., 2013. Treatment of petroleum refinery sulfidic spent caustic wastes by electrocoagulation. *Sep. Purif. Technol.* 107, 150–157. <https://doi.org/10.1016/j.seppur.2013.01.051>
- Huang, K.C., Zhao, Z., Hoag, G.E., Dahmani, A., Block, P. a., 2005. Degradation of volatile organic compounds with thermally activated persulfate oxidation. *Chemosphere* 61, 551–560. <https://doi.org/10.1016/j.chemosphere.2005.02.032>
- Ike, I.A., Linden, K., Orbell, J.D., Duke, M., 2018. Critical review of the science and sustainability of persulphate advanced oxidation processes, *Chemical Engineering Journal*. Elsevier B.V. <https://doi.org/10.1016/j.cej.2018.01.034>
- Katsoyiannis, I.A., Canonica, S., von Gunten, U., 2011. Efficiency and energy requirements for the transformation of organic micropollutants by ozone, O<sub>3</sub>/H<sub>2</sub>O<sub>2</sub> and UV/H<sub>2</sub>O<sub>2</sub>. *Water Res.* 45, 3811–3822.



<https://doi.org/10.1016/j.watres.2011.04.038>

- Khan, J.A., He, X., Khan, H.M., Shah, N.S., Dionysiou, D.D., 2013. Oxidative degradation of atrazine in aqueous solution by UV/H<sub>2</sub>O<sub>2</sub>/Fe<sup>2+</sup>, UV/S<sub>2</sub>O<sub>8</sub><sup>2-</sup>/Fe<sup>2+</sup> and UV/HSO<sub>5</sub><sup>-</sup>/Fe<sup>2+</sup> processes: A comparative study. *Chem. Eng. J.* 218, 376-383. <https://doi.org/10.1016/j.cej.2012.12.055>
- Khan, J.A., He, X., Shah, N.S., Khan, H.M., Hapeshi, E., Fatta-Kassinos, D., Dionysiou, D.D., 2014. Kinetic and mechanism investigation on the photochemical degradation of atrazine with activated H<sub>2</sub>O<sub>2</sub>, S<sub>2</sub>O<sub>8</sub><sup>2-</sup> and HSO<sub>5</sub><sup>-</sup>. *Chem. Eng. J.* 252, 393-403. <https://doi.org/10.1016/j.cej.2014.04.104>
- Khan, J.A., He, X., Shah, N.S., Sayed, M., Khan, H.M., Dionysiou, D.D., 2017. Degradation kinetics and mechanism of desethyl-atrazine and desisopropyl-atrazine in water with •OH and SO<sub>4</sub><sup>•-</sup> based-AOPs. *Chem. Eng. J.* 325, 485-494. <https://doi.org/10.1016/j.cej.2017.05.011>
- Kim, S.B., Hong, S.C., 2002. Kinetic study for photocatalytic degradation of volatile organic compounds in air using thin film TiO<sub>2</sub> photocatalyst. *Appl. Catal. B Environ.* 35, 305–315. [https://doi.org/10.1016/S0926-3373\(01\)00274-0](https://doi.org/10.1016/S0926-3373(01)00274-0)
- Kusic, H., Koprivanac, N., Bozic, A.L., 2006. Minimization of organic pollutant content in aqueous solution by means of AOPs: UV- and ozone-based technologies. *Chem. Eng. J.* 123, 127–137. <https://doi.org/10.1016/j.cej.2006.07.011>
- Kwok, E.S.C., Atkinson, R., 1995. Estimation of hydroxyl radical reaction rate constants for gas phase organic compounds using a structure-reactivity relationship: An update. *Atmos. Environ.* 29, 1685–1695. [https://doi.org/10.1016/1352-2310\(95\)00069-B](https://doi.org/10.1016/1352-2310(95)00069-B)
- Li, W., Niu, Q., Zhang, H., Tian, Z., Zhang, Y., Gao, Y., Li, Y.Y., Nishimura, O., Yang, M., 2014. UASB treatment of chemical synthesis-based pharmaceutical wastewater containing rich organic sulfur compounds and sulfate and associated microbial characteristics. *Chem. Eng. J.* 260, 55–63. <https://doi.org/10.1016/j.cej.2014.08.085>
- Liang, X., Zhu, X., Butler, E.C., 2011. Comparison of four advanced oxidation processes for the removal of naphthenic acids from model oil sands process water. *J. Hazard. Mater.* 190, 168–176. <https://doi.org/10.1016/j.jhazmat.2011.03.022>
- Litter, M., 2005. Introduction to Photochemical Advanced Oxidation Processes for Water Treatment, in: Boule, P., Bahnemann, D.W., Robertson, P.K.J. (Eds.), *Environmental Photochemistry Part II*. Springer Berlin Heidelberg, pp. 325–366. <https://doi.org/10.1007/b89482>
- Liu, X., Zhang, T., Zhou, Y., Fang, L., Shao, Y., 2013. Degradation of atenolol by UV/peroxymonosulfate: Kinetics, effect of operational parameters and mechanism. *Chemosphere* 93, 2717–2724. <https://doi.org/10.1016/j.chemosphere.2013.08.090>
- Long, A., Lei, Y., Zhang, H., 2014. Degradation of Toluene by a Selective Ferrous Ion Activated Persulfate Oxidation Process. *Ind. Eng. Chem. Res.* 53, 1033–1039. <https://doi.org/10.1021/ie402633n>
- Matzek, L.W., Carter, K.E., 2016. Activated persulfate for organic chemical degradation: A review. *Chemosphere* 151, 178–188.

<https://doi.org/10.1016/j.chemosphere.2016.02.055>

- Neta, P., Huie, R.E., Ross, A.B., 1988. Rate constants for reactions of inorganic radicals in aqueous solution. *J. Phys. Chem. Ref. Data* 17, 1027–1040.
- Ning, X.A., Wang, J.Y., Li, R.J., Wen, W. Bin, Chen, C.M., Wang, Y.J., Yang, Z.Y., Liu, J.Y., 2015. Fate of volatile aromatic hydrocarbons in the wastewater from six textile dyeing wastewater treatment plants. *Chemosphere* 136, 50–55. <https://doi.org/10.1016/j.chemosphere.2015.03.086>
- Oh, S.-Y., Shin, D.-S., 2013. Treatment of Diesel-Contaminated Soil by Fenton and Persulfate Oxidation with Zero-Valent Iron. *Soil Sediment Contam. An Int. J.* 23, 180–193. <https://doi.org/10.1080/15320383.2014.808170>
- Oh, S.Y., Kang, S.G., Kim, D.W., Chiu, P.C., 2011. Degradation of 2,4-dinitrotoluene by persulfate activated with iron sulfides. *Chem. Eng. J.* 172, 641–646. <https://doi.org/10.1016/j.cej.2011.06.023>
- Ojala, S., Pitkääho, S., Laitinen, T., Niskala Koivikko, N., Brahmi, R., Gaálová, J., Matejova, L., Kucherov, A., Päivärinta, S., Hirschmann, C., Nevanperä, T., Riihimäki, M., Pirilä, M., Keiski, R.L., 2011. Catalysis in VOC Abatement. *Top. Catal.* 54, 1224–1256. <https://doi.org/10.1007/s11244-011-9747-1>
- Patnaik, P., Khoury, J.N., 2004. Reaction of phenol with nitrite ion: Pathways of formation of nitrophenols in environmental waters. *Water Res.* 38, 206–210. <https://doi.org/10.1016/j.watres.2003.08.022>
- Popiel, S., Nalepa, T., Dzierzak, D., Stankiewicz, R., Witkiewicz, Z., 2009. Rate of dibutylsulfide decomposition by ozonation and the O<sub>3</sub>/H<sub>2</sub>O<sub>2</sub> advanced oxidation process. *J. Hazard. Mater.* 164, 1364–1371. <https://doi.org/10.1016/j.jhazmat.2008.09.049>
- Poyatos, J.M., Muñio, M.M., Almecija, M.C., Torres, J.C., Hontoria, E., Osorio, F., 2010. Advanced Oxidation Processes for Wastewater Treatment: State of the Art. *Water. Air. Soil Pollut.* 205, 187–204. <https://doi.org/10.1007/s11270-009-0065-1>
- Qi, C., Liu, X., Ma, J., Lin, C., Li, X., Zhang, H., 2016. Activation of peroxymonosulfate by base: Implications for the degradation of organic pollutants. *Chemosphere* 151, 280–288. <https://doi.org/10.1016/j.chemosphere.2016.02.089>
- Rehman, F., Sayed, M., Khan, J.A., Shah, N.S., Khan, H.M., Dionysiou, D.D., 2018. Oxidative removal of brilliant green by UV/S<sub>2</sub>O<sub>8</sub><sup>2-</sup>, UV/HSO<sub>5</sub><sup>-</sup> and UV/H<sub>2</sub>O<sub>2</sub> processes in aqueous media: A comparative study. *J. Hazard. Mater.* 357, 506–514. <https://doi.org/10.1016/j.jhazmat.2018.06.012>
- Ren, X., Zeng, G., Tang, L., Wang, J., Wan, J., Feng, H., Song, B., Huang, C., Tang, X., 2018. Effect of exogenous carbonaceous materials on the bioavailability of organic pollutants and their ecological risks. *Soil Biol. Biochem.* 116, 70–81. <https://doi.org/10.1016/j.soilbio.2017.09.027>
- Rigol, A., Latorre, A., Lacorte, S., Barceló, D., 2002. Determination of toxic compounds in paper-recycling process waters by gas chromatography-mass spectrometry and liquid chromatography-mass spectrometry. *J. Chromatogr. A* 963, 265–275. [https://doi.org/10.1016/S0021-9673\(02\)00232-7](https://doi.org/10.1016/S0021-9673(02)00232-7)
- Safarzadeh-Amiri, A., 2001. O<sub>3</sub>/H<sub>2</sub>O<sub>2</sub> treatment of methyl-tert-butyl ether (MTBE) in

contaminated waters. *Water Res.* 35, 3706–3714. [https://doi.org/10.1016/S0043-1354\(01\)00090-2](https://doi.org/10.1016/S0043-1354(01)00090-2)

Saien, J., Nejati, H., 2007. Enhanced photocatalytic degradation of pollutants in petroleum refinery wastewater under mild conditions. *J. Hazard. Mater.* 148, 491–495. <https://doi.org/10.1016/j.jhazmat.2007.03.001>

Saien, J., Shahrezaei, F., 2012. Organic Pollutants Removal from Petroleum Refinery Wastewater with Nanotitania Photocatalyst and UV Light Emission. *Int. J. Photoenergy* 2012, 1–5. <https://doi.org/10.1155/2012/703074>

Sato, K., Hyodo, M., Aoki, M., Zheng, X.Q., Noyori, R., 2001. Oxidation of sulfides to sulfoxides and sulfones with 30% hydrogen peroxide under organic solvent- and halogen-free conditions. *Tetrahedron* 57, 2469–2476. [https://doi.org/10.1016/S0040-4020\(01\)00068-0](https://doi.org/10.1016/S0040-4020(01)00068-0)

Sayed, M., Khan, J.A., Shah, L.A., Shah, N.S., Shah, F., Khan, H.M., Zhang, P., Arandiyani, H., 2018. Solar Light Responsive Poly(vinyl alcohol)-Assisted Hydrothermal Synthesis of Immobilized TiO<sub>2</sub>/Ti Film with the Addition of Peroxymonosulfate for Photocatalytic Degradation of Ciprofloxacin in Aqueous Media: A Mechanistic Approach. *J. Phys. Chem. C* 122, 406–421. <https://doi.org/10.1021/acs.jpcc.7b09169>

Shah, N.S., Khan, J.A., Sayed, M., Khan, Z.U.H., Rizwan, A.D., Muhammad, N., Boczkaj, G., Murtaza, B., Imran, M., Khan, H.M., Zaman, G., 2018a. Solar light driven degradation of norfloxacin using as-synthesized Bi<sup>3+</sup> and Fe<sup>2+</sup> co-doped ZnO with the addition of HSO<sub>5</sub><sup>-</sup>: Toxicities and degradation pathways investigation. *Chem. Eng. J.* 351, 841–855. <https://doi.org/10.1016/j.cej.2018.06.111>

Shah, N.S., Rizwan, A.D., Khan, J.A., Sayed, M., Khan, Z.U.H., Murtaza, B., Iqbal, J., Din, S.U., Imran, M., Nadeem, M., Al-Muhtaseb, A.H., Muhammad, N., Khan, H.M., Ghauri, M., Zaman, G., 2018b. Toxicities, kinetics and degradation pathways investigation of ciprofloxacin degradation using iron-mediated H<sub>2</sub>O<sub>2</sub> based advanced oxidation processes. *Process Saf. Environ. Prot.* 117, 473–482. <https://doi.org/10.1016/j.psep.2018.05.020>

Shahidi, D., Roy, R., Azzouz, A., 2015. Advances in catalytic oxidation of organic pollutants – Prospects for thorough mineralization by natural clay catalysts. *Appl. Catal. B Environ.* 174–175, 277–292. <https://doi.org/10.1016/j.apcatb.2015.02.042>

Sharma, J., Mishra, I.M., Dionysiou, D.D., Kumar, V., 2015. Oxidative removal of Bisphenol A by UV-C/peroxymonosulfate (PMS): Kinetics, influence of co-existing chemicals and degradation pathway. *Chem. Eng. J.* 276, 193–204. <https://doi.org/10.1016/j.cej.2015.04.021>

Shen, Y.-S., Ku, Y., 1999. Treatment of gas-phase volatile organic compounds (VOCs) by the process. *Chemosphere* 38, 1855–1866. [https://doi.org/10.1016/S0045-6535\(98\)00400-7](https://doi.org/10.1016/S0045-6535(98)00400-7)

Sipma, J., Svitelskaya, A., Mark, B. Van Der, Hulshoff, L.W., Lettinga, G., Buisman, C.J.N., Janssen, A.J.H., 2004. Potentials of biological oxidation processes for the treatment of spent sulfidic caustics containing thiols. *Water Res.* 38, 4331–4340. <https://doi.org/10.1016/j.watres.2004.08.022>

Spalek, O., Balej, J., Paseka, I., 1982. Kinetics of the decomposition of hydrogen

peroxide in alkaline solutions. *J. Chem. Soc. Faraday Trans.* 78, 2349.  
<https://doi.org/10.1039/f19827802349>

- Stepnowski, P., Siedlecka, E.M., Behrend, P., Jastorff, B., 2002. Enhanced photo-degradation of contaminants in petroleum refinery wastewater. *Water Res.* 36, 2167–2172.
- Sun, R., Lawther, J.M., Banks, W.B., 1995. The effect of alkaline nitrobenzene oxidation conditions on the yield and components of phenolic monomers in wheat straw lignin and compared to cupric(II) oxidation. *Ind. Crops Prod.* 4, 241–254.  
[https://doi.org/10.1016/0926-6690\(95\)00038-0](https://doi.org/10.1016/0926-6690(95)00038-0)
- Ventura, A., Lorino, T., Le Guen, L., 2015. Modeling of Polycyclic Aromatic Hydrocarbons stack emissions from a hot mix asphalt plant for gate-to-gate Life Cycle Inventory. *J. Clean. Prod.* 93, 151–158.  
<https://doi.org/10.1016/j.jclepro.2015.01.021>
- Vione, D., Maurino, V., Minero, C., Pelizzetti, E., 2001. Phenol photolysis upon UV irradiation of nitrite in aqueous solution I: Effects of oxygen and 2-propanol. *Chemosphere* 45, 893–902. [https://doi.org/10.1016/S0045-6535\(01\)00035-2](https://doi.org/10.1016/S0045-6535(01)00035-2)
- von Sonntag, C. (Ed.), 2005. Free-radical-induced DNA damage and its repair- A chemical perspective. Springer, Berlin Heidelberg.
- Wacławek, S., Lutze, H. V, Grübel, K., Padil, V.V., Černík, M., Dionysiou, D., 2017. Chemistry of persulfates in water and wastewater treatment: A review. *Chem. Eng. J.* 330, 44–62. <https://doi.org/10.1016/j.cej.2017.07.132>
- Wols, B.A., Hofman-Caris, C.H.M., Harmsen, D.J.H., Beerendonk, E.F., 2013. Degradation of 40 selected pharmaceuticals by UV/H<sub>2</sub>O<sub>2</sub>. *Water Res.* 47, 5876–5888. <https://doi.org/10.1016/j.watres.2013.07.008>
- Wright, S.W., Abelman, M.M., Bostrom, L.L., Corbett, R.L., 1992. Benzyl and t-butyl sulfoxides as sulfenyl halide equivalents: a convenient preparation of benzisothiazolones. *Tetrahedron Lett.* 33, 153–156. [https://doi.org/10.1016/0040-4039\(92\)88037-6](https://doi.org/10.1016/0040-4039(92)88037-6)
- Wu, J.J., Muruganandham, M., Chen, S.H., 2007. Degradation of DMSO by ozone-based advanced oxidation processes. *J. Hazard. Mater.* 149, 218–225.  
<https://doi.org/10.1016/j.jhazmat.2007.03.071>
- Zheng, Y., Hill, D.O., Kuo, C.H., 1993. Destruction of cresols by chemical oxidation. *J. Hazard. Mater.* 34, 245–260. [https://doi.org/10.1016/0304-3894\(93\)85009-4](https://doi.org/10.1016/0304-3894(93)85009-4)

Table 1 – Operational parameters of each process studied

Process	t (min)	Amount Oxidant (g)	T (°C)
H <sub>2</sub> O <sub>2</sub>	182	31	40
H <sub>2</sub> O <sub>2</sub>	181.5	62	40
O <sub>3</sub>	220	35	40
O <sub>3</sub>	356	69	40
O <sub>3</sub> /H <sub>2</sub> O <sub>2</sub>	250	98 (O <sub>3</sub> : 48.5; H <sub>2</sub> O <sub>2</sub> : 49.5)	40
O <sub>3</sub> /H <sub>2</sub> O <sub>2</sub>	317	189 (O <sub>3</sub> : 61.5, H <sub>2</sub> O <sub>2</sub> : 127.5)	40
PS	182	218	40
PS	182	436	40
PS	182	218	60
PS	182	436	60
PMS	139	114	40
PMS	139	114	60
PMS	182	70	40
PMS	182	70	60



Table 2 – Effectiveness of degradation of each model compound using classic AOPs, i.e., H<sub>2</sub>O<sub>2</sub>, O<sub>3</sub> and O<sub>3</sub>/H<sub>2</sub>O<sub>2</sub>.

Compound	primary conc. (mg/L)	Classic AOPs					
		H <sub>2</sub> O <sub>2</sub> 31 g	H <sub>2</sub> O <sub>2</sub> 62 g	O <sub>3</sub> 35 g	O <sub>3</sub> 69 g	O <sub>3</sub> /H <sub>2</sub> O <sub>2</sub> 98 g (O <sub>3</sub> = 48.5; H <sub>2</sub> O <sub>2</sub> = 49.5)	O <sub>3</sub> /H <sub>2</sub> O <sub>2</sub> 189 g (O <sub>3</sub> = 61.5; H <sub>2</sub> O <sub>2</sub> = 127.5)
Benzene	8.87	80.0%	96.5%	99.3%	99.5%	100%	100%
Toluene	8.73	76.4%	95.1%	99.7%	99.9%	100%	>99.9%
o-xylene	10.05	70.4%	94.3%	>99.9%	>99.9%	>99.9%	>99.9%
2-ethylthiophene	8.64	56.1%	94.2%	>99.8%	>99.8%	>99.9%	>99.8%
Ethylbenzene	9.45	63.7%	92.6%	>99.9%	>99.9%	>99.9%	>99.9%
2-ethyl-1-hexanol	9.35	49.1%	99.9%	>99.9%	>99.9%	>99.9%	>99.9%
Phenol	9.37	72.5%	98.7%	99.4%	99.6%	>99.9%	>99.9%
Dibutyl sulfide	10.92	>99.7%	>99.8%	>99.7%	>99.7%	>99.7%	>99.8%
4-methylbenzaldehyde	9.98	-89.2%	67.4%	100%	95.2%	100%	100%
Nitrobenzene	9.70	9.4%	61.2%	94.2%	99.8%	>99.8%	>99.8%
4-ethylphenol	9.69	42.8%	>99.8%	>99.9%	>99.8%	>99.9%	>99.9%
2-Nitrotoluene	10.13	11.7%	73.8%	98.2%	>99.9%	>99.9%	>99.8%
Naphthalene	9.77	60.8%	85.5%	99.3%	99.3%	>99.9%	100%
di-tert-butyl disulfide	11.90	-45.1%	>99.0%	>98.6%	>98.8%	>98.5%	>99.0%
2-nitrophenol	9.78	-444.7%	-121.6%	92.8%	>99.8%	>99.8%	>99.8%
2,6-dimethylphenol	9.18	44.7%	>99.8%	84.6%	>99.8%	>99.8%	>99.8%
Total O-VOCs	94.44	47.1%	91.4%	98.3%	99.3%	100%	100%
Total VSCs	31.46	36.4%	98.7%	100%	100%	100%	100%
Total VNCs	29.61	-139.1%	-2.2%	95.1%	99.9%	100%	100%
Total VOCS	155.51	10.7%	74.7%	98.0%	99.6%	100.0%	100.0%



Table 3 - Effectiveness of degradation of each model compound using S-AOPs, i.e., Na<sub>2</sub>S<sub>2</sub>O<sub>8</sub> and KHSO<sub>5</sub>.

Compound	primary conc. (mg/L)	Sulfate related AOPs							
		Na <sub>2</sub> S <sub>2</sub> O <sub>8</sub> 218 g 40 °C	Na <sub>2</sub> S <sub>2</sub> O <sub>8</sub> 436 g 40 °C	Na <sub>2</sub> S <sub>2</sub> O <sub>8</sub> 218 g 60 °C	Na <sub>2</sub> S <sub>2</sub> O <sub>8</sub> 436 g 60 °C	KHSO <sub>5</sub> 114 g 40 °C	KHSO <sub>5</sub> 114 g 60 °C	KHSO <sub>5</sub> 70 g 40 °C	KHSO <sub>5</sub> 70 g 60 °C
Benzene	11.24	91.0%	95.6%	97.4%	98.8%	76.2%	85.0%	47.0%	93.2%
Toluene	9.60	82.1%	85.4%	90.4%	94.7%	76.4%	89.7%	18.0%	82.4%
o-xylene	10.01	88.5%	92.7%	96.0%	97.4%	85.2%	85.5%	-13.5%	87.3%
2-ethylthiophene	10.04	95.5%	99.9%	99.9%	99.9%	10.8%	99.9%	93.3%	99.8%
Ethylbenzene	12.01	91.2%	92.2%	94.9%	96.9%	85.0%	81.2%	29.2%	91.5%
2-Ethyl-1-hexanol	13.57	56.6%	98.5%	99.2%	100%	55.4%	79.9%	0.4%	96.7%
Phenol	8.46	98.0%	96.0%	99.9%	99.9%	99.9%	99.9%	99.9%	99.9%
Dibutyl sulfide	15.35	60.0%	99.8%	99.8%	99.7%	99.8%	99.8%	95.4%	99.8%
4-methylbenzaldehyde	13.52	3.4%	100%	98.6%	100%	80.1%	100%	73.9%	97.4%
Nitrobenzene	8.87	-12.3%	65.9%	65.0%	99.8%	11.9%	1.3%	0.2%	83.7%
4-ethylphenol	10.00	98.9%	99.9%	99.8%	99.9%	99.9%	99.9%	99.9%	99.9%
2-nitrotoluene	7.81	-26.2%	21.2%	76.4%	87.4%	12.7%	1.6%	1.9%	77.5%
Naphthalene	11.21	37.1%	100%	100%	100%	96.9%	100%	33.2%	99.9%
di-tert-butylsulfide	15.29	99.0%	99.1%	99.0%	98.8%	99.2%	98.4%	98.0%	98.5%
2-nitrophenol	11.40	99.9%	99.8%	99.8%	99.9%	99.9%	99.9%	99.8%	99.8%

2,6-dimethylphenol	6.22	99.7%	99.7%	99.6%	99.7%	99.7%	99.7%	85.9%	99.7%
Total O-VOCs	105.84	70.6%	96.3%	97.7%	98.7%	83.9%	90.6%	56.8%	95.7%
Total VSCs	40.68	83.5%	100%	100%	100%	79.9%	100%	96.2%	100%
Total VNCs	28.08	33.0%	67.7%	82.4%	96.8%	49.4%	46.9%	44.5%	88.6%
Total VOCS	174.60	67.2%	92.9%	95.7%	98.6%	77.2%	84.8%	64.8%	95.6%

Table 4 – Summary of the treatment cost calculations for the AOPs studied. \$ represents American dollars.

AOP	Treatment time (min)	Oxidant amount (g)	T (°C)	Treatment time for effective VOCs degradation (min)	Oxidant amount for effective VOCs degradation(g)	Chemical cost (\$)	Energy demand (kJ)	Energy cost (\$)	Total cost (\$)	Treatment cost (\$/L)
H <sub>2</sub> O <sub>2</sub>	181.5	31	40	181.5	31.11	0.05	871.2	0.03	0.07	0.01
H <sub>2</sub> O <sub>2</sub>	181.5	62	40	181.5	62.23	0.09	871.2	0.03	0.12	0.02
O <sub>3</sub>	220.2	35	40	120	18.9	-	3240	0.10	0.10	0.02
O <sub>3</sub>	357.6	70	40	357.6	69.38	-	9655.2	0.30	0.30	0.06
O <sub>3</sub> /H <sub>2</sub> O <sub>2</sub>	250.1	O <sub>3</sub> 48.5 H <sub>2</sub> O <sub>2</sub> 49.5	40	30	O <sub>3</sub> 5.82 H <sub>2</sub> O <sub>2</sub> 5.93	0.01	954	0.03	0.04	0.01
O <sub>3</sub> /H <sub>2</sub> O <sub>2</sub>	317.1	O <sub>3</sub> 61.5 H <sub>2</sub> O <sub>2</sub> 127.5	40	30	O <sub>3</sub> 5.82 H <sub>2</sub> O <sub>2</sub> 12.05	0.02	954	0.03	0.05	0.01
Na <sub>2</sub> S <sub>2</sub> O <sub>8</sub>	181.5	218	40	181.5	217.79	8.87	871.2	0.03	8.90	1.78
-										
Na <sub>2</sub> S <sub>2</sub> O <sub>8</sub>	181.5	436	40	181.5	435.59	17.75	871.2	0.03	17.77	3.55
-										
Na <sub>2</sub> S <sub>2</sub> O <sub>8</sub>	181.5	218	60	120	144	5.87	576	0.02	5.88	1.18
-										
Na <sub>2</sub> S <sub>2</sub> O <sub>8</sub>	181.5	436	60	120	288	11.73	576	0.02	11.75	2.35
-										
KHSO <sub>5</sub>	138.7	114	40	138.7	114.3	6.47	665.76	0.02	6.49	1.30
KHSO <sub>5</sub>	138.7	114	60	138.7	114.3	6.47	665.76	0.02	6.49	1.30
KHSO <sub>5</sub>	181.5	70	40	181.5	69.67	3.94	871.2	0.03	3.97	0.79
KHSO <sub>5</sub>	181.5	70	60	120	46.08	2.61	576	0.02	2.62	0.52



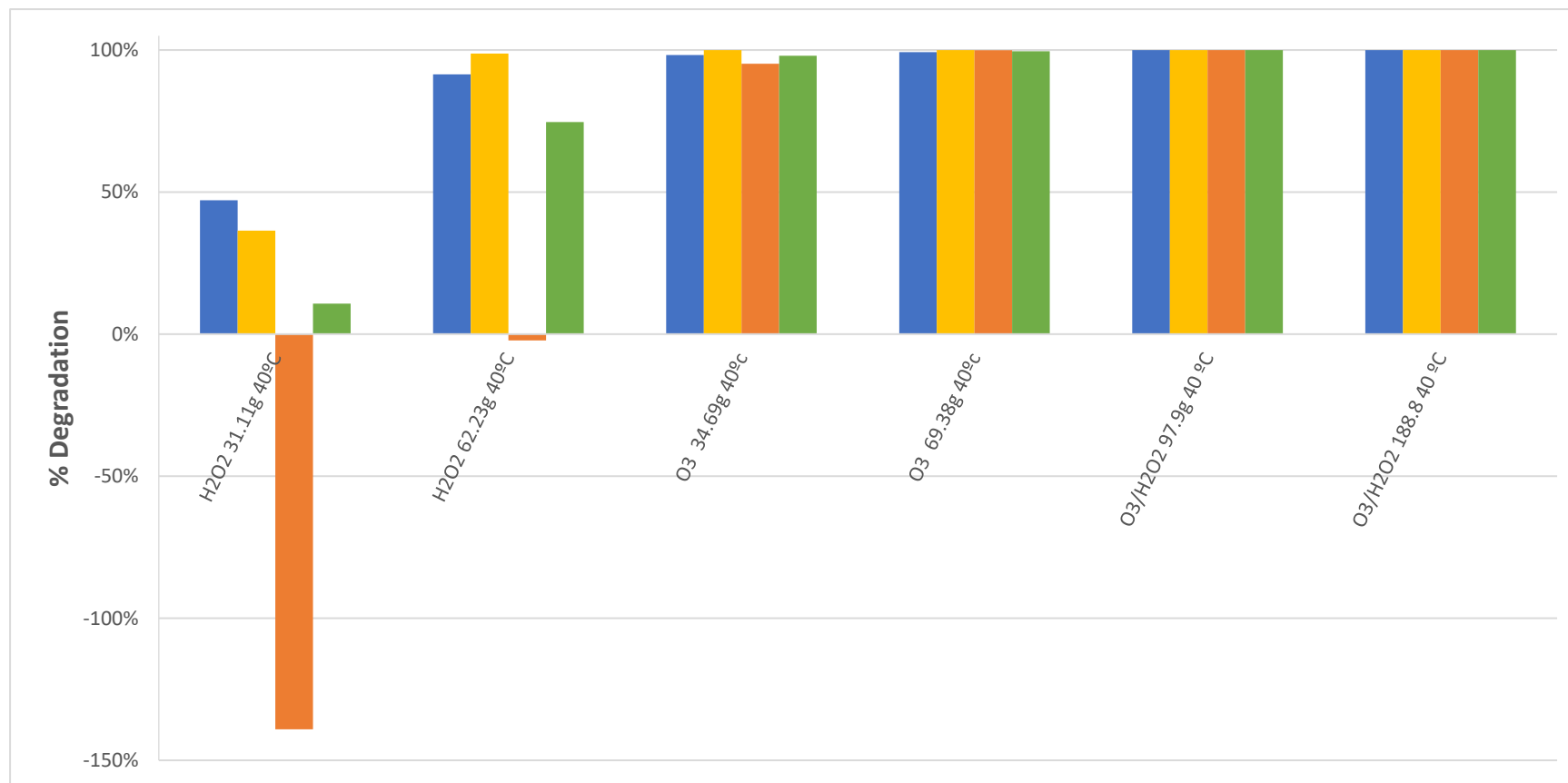


Figure 1 – total O-VOCs, VSCs, VNCs and total VOCs degradation for the classic AOPs. Blue bars, total O-VOCs; yellow bars total VSCs, orange bars, VNCs, green bars, total VOCs.

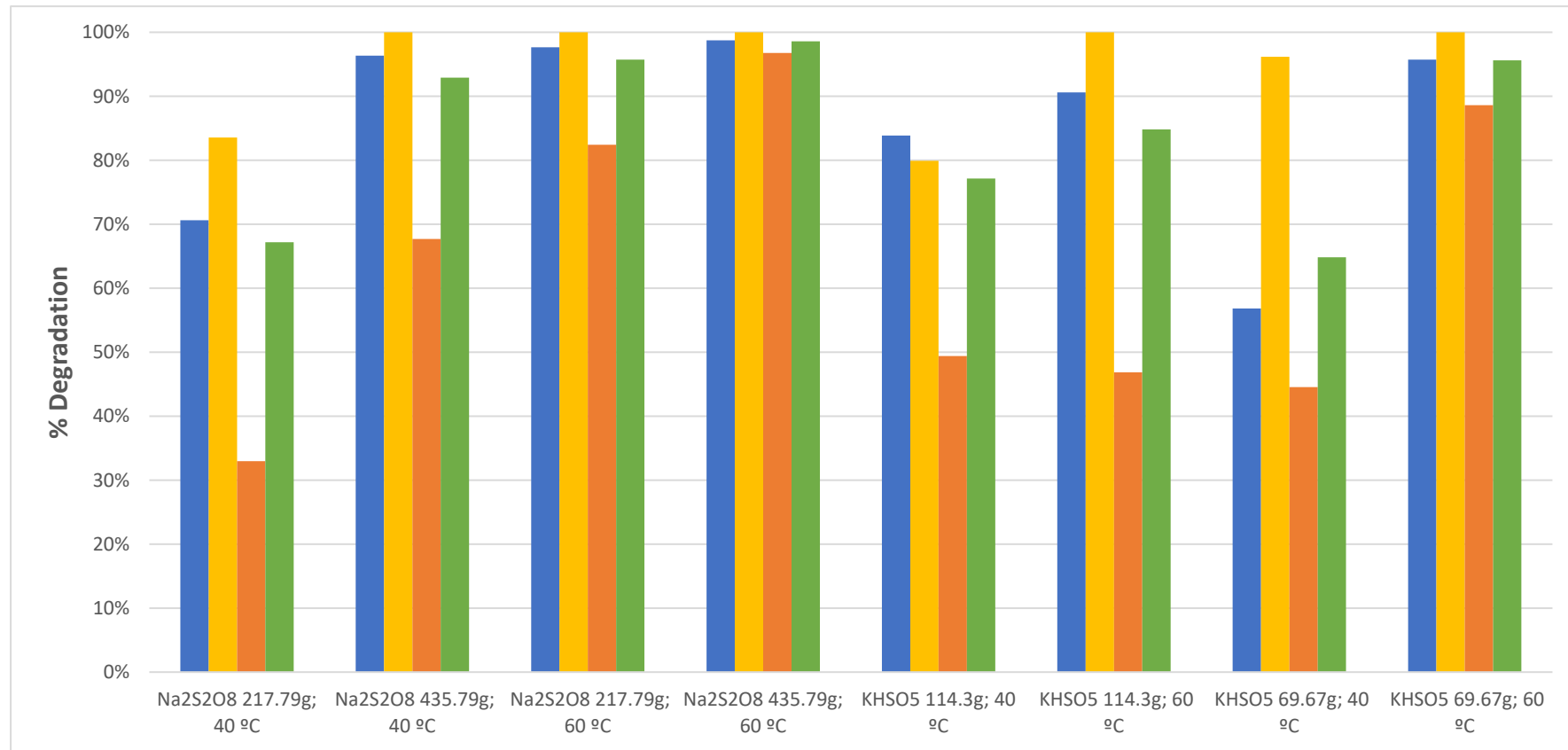


Figure 2 – total O-VOCs, VSCs, VNCs and total VOCs degradation for the S-AOPs. Blue bars, total O-VOCs; yellow bars total VSCs, orange bars, VNCs, green bars, total VOCs.

**Pilot scale degradation study of 16 selected volatile organic compounds  
by hydroxyl and sulfate radical based Advanced Oxidation Processes**

**Supporting Information**

*André Fernandes<sup>1</sup>, Patrycja Makoś<sup>1</sup>, Javed Ali Khan<sup>2</sup>, Grzegorz Boczkaj<sup>1,\*</sup>*

<sup>1</sup>Gdansk University of Technology, Faculty of Chemistry, Department of Chemical and Process Engineering, 80 – 233 Gdansk, G. Narutowicza St. 11/12, Poland

<sup>2</sup>Radiation Chemistry Laboratory, National Centre of Excellence in Physical Chemistry, University of Peshawar, Peshawar 25120, Pakistan

*\* Corresponding author: Dr Grzegorz Boczkaj, PhD. Sc. Eng. Fax: (+48 58) 347-26-94; Tel: (+48) 697970303; E-mail: grzegorz.boczkaj@gmail.com or grzegorz.boczkaj@pg.edu.pl*



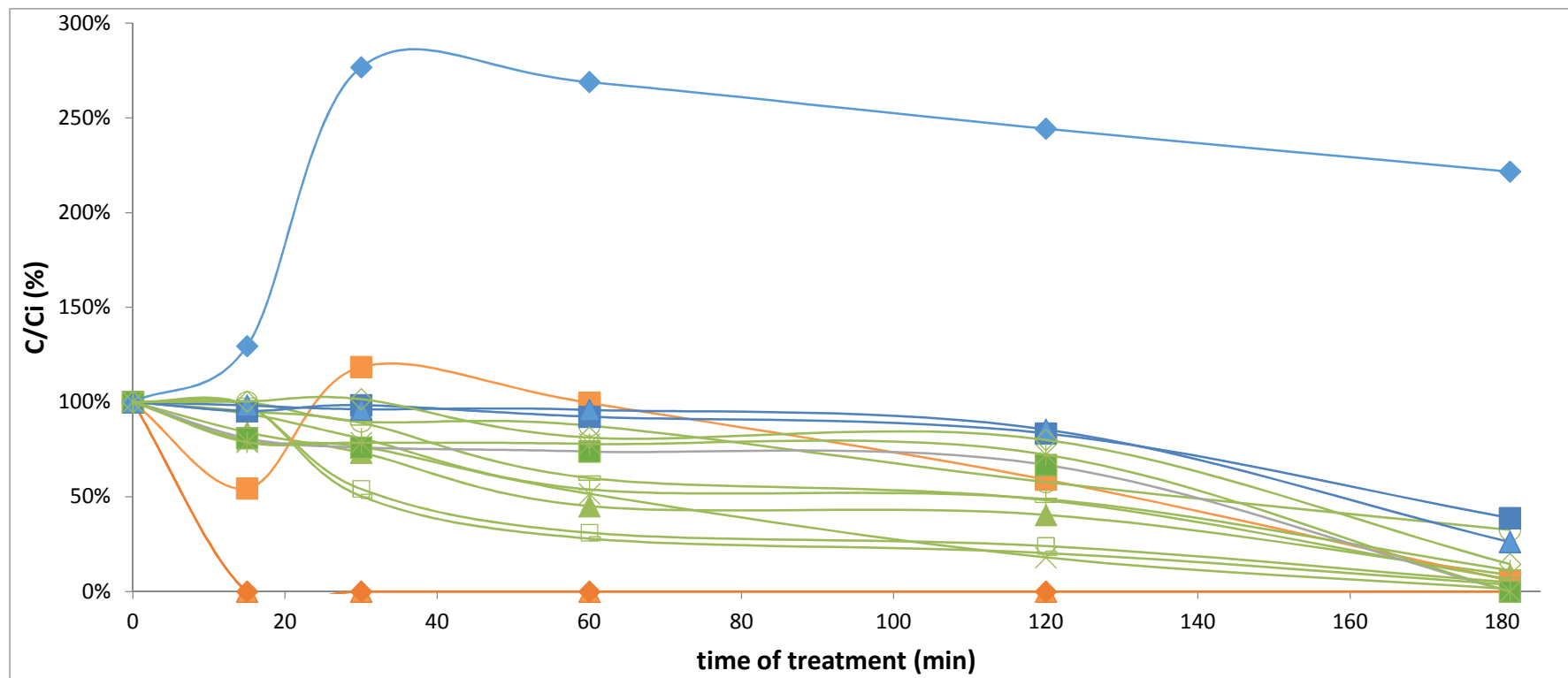


Figure 1S – VOCs degradation profile during the oxidation for H<sub>2</sub>O<sub>2</sub> process at 40 °C with a dose of 62 g. Green empty squares, toluene; green plus, ethylbenzene; empty green circles, 4-methylbenzaldehyde; green dots, benzene; green traces, 2-ethyl-1-hexanol; solid green triangles, o-xylene; green crosses, phenol; solid green squares, 4-ethylphenol; green star, 2,6-dimethylphenol; empty green diamonds, naphthalene; solid blue diamonds, 2-nitrophenol; solid blue triangles, 2-nitrotoluene; solid blue squares, nitrobenzene; solid orange diamonds, di-tert-butyl disulfide; solid orange squares, 2-ethylthiophene; solid orange triangles, dibutyl sulfide.



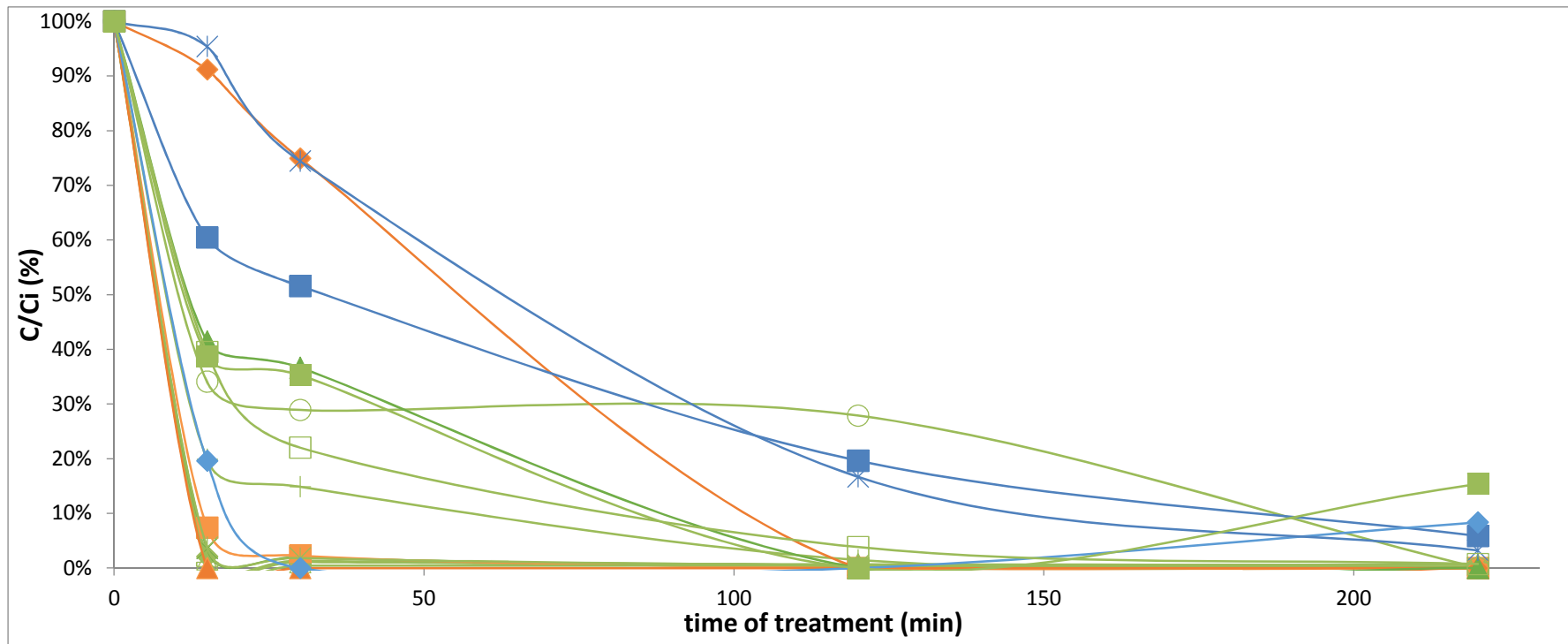


Figure 2S- VOCs degradation profile during the oxidation time for O<sub>3</sub> process at 40 °C with a dose of 35 g. Solid green diamonds, toluene; green stars, ethylbenzene; empty green circles, 4-methylbenzaldehyde; empty green triangles, benzene; green plus, 2-ethyl-1-hexanol; green crosses, o-xylene; green traces, phenol; solid green squares, 2,6-dimethylphenol; solid green triangles – 4-ethylphenol; empty green squares, naphthalene; solid blue diamonds, 2-nitrophenol; blue stars, 2-nitrotoluene; solid blue squares, nitrobenzene; solid orange diamonds, di-tert-butyl disulfide; solid orange squares, 2-ethylthiophene; solid orange triangles, dibutyl sulfide.





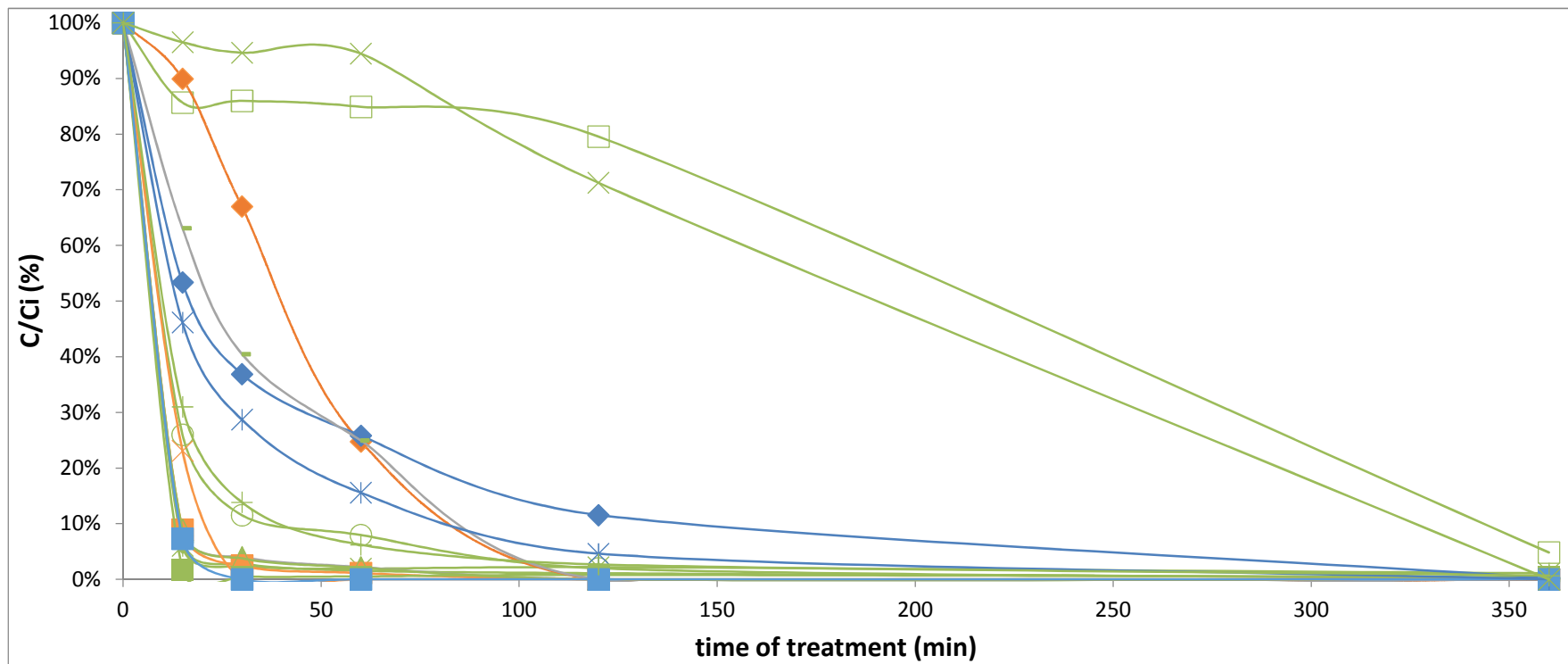


Figure 3S - VOCs degradation profile during the oxidation time for  $O_3$  process at 40 °C with a dose of 70 g. Solid green diamonds, toluene; empty green triangles, ethylbenzene; empty green squares, 4-methylbenzaldehyde; green stars, benzene; empty green circles, 2-ethyl-1-hexanol; solid green triangles, o-xylene; solid green squares, phenol; green crosses, 2,6-dimethylphenol; green dots – 4-ethylphenol; green pluses, naphthalene; solid blue squares, 2-nitrophenol; blue stars, 2-nitrotoluene; solid blue diamonds, nitrobenzene; solid orange diamonds, di-tert-butyl disulfide; solid orange squares, 2-ethylthiophene; orange crosses, dibutyl sulfide.



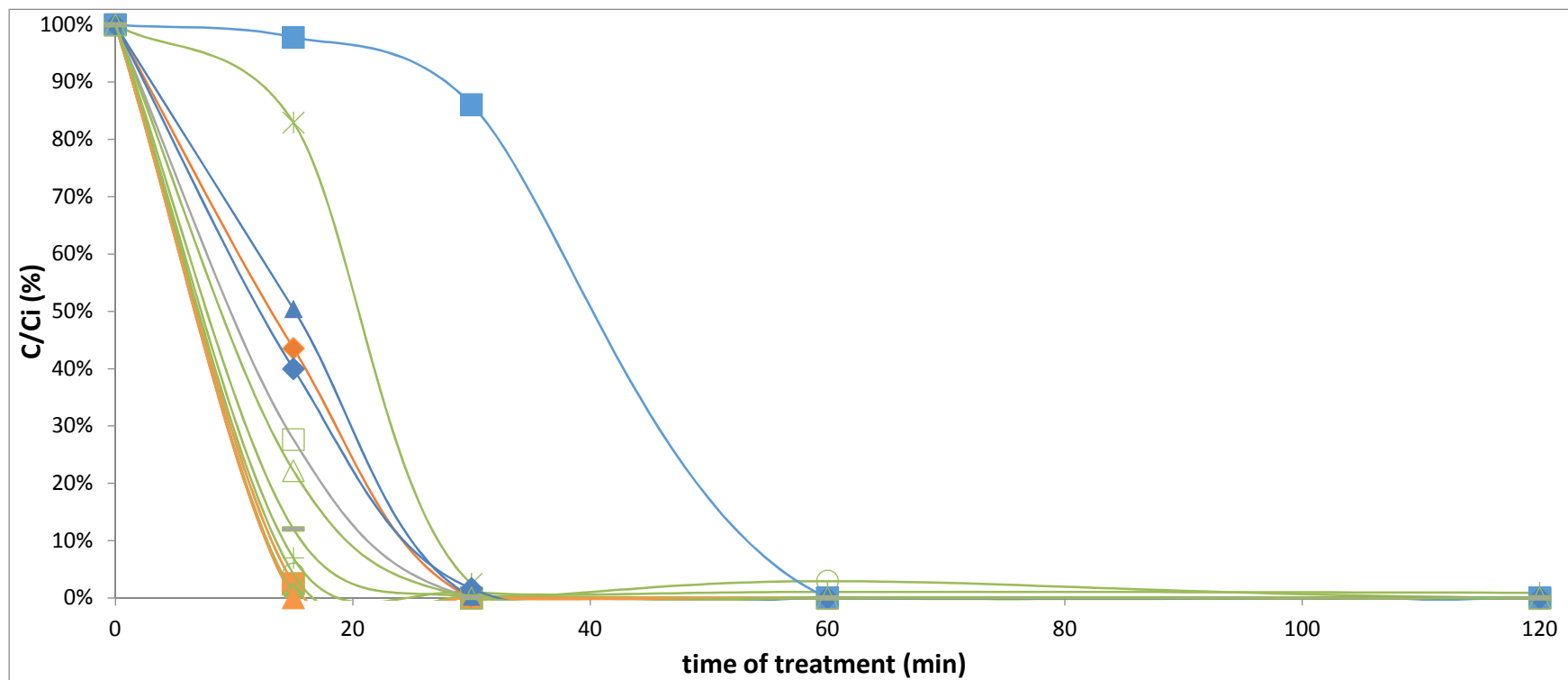


Figure 4S - - VOCs degradation profile during the oxidation time for  $O_3/H_2O_2$  process at 40 °C with a dose of 98 g ( $O_3 = 48.5$ ,  $H_2O_2 = 49.5$ ). Solid green squares, toluene; empty green circles, ethylbenzene; green stars, 4-methylbenzaldehyde; solid green triangles, benzene; green plus, 2-ethyl-1-hexanol; green crosses, o-xylene; solid green diamonds, phenol; empty green triangles, 2,6-dimethylphenol; empty green squares – 4-ethylphenol; green traces, naphthalene; solid blue squares, 2-nitrophenol; solid blue diamonds, 2-nitrotoluene; solid blue triangles, nitrobenzene; solid orange diamonds, di-tert-butyl disulfide; solid orange squares, 2-ethylthiophene; solid orange triangles, dibutyl sulfide.

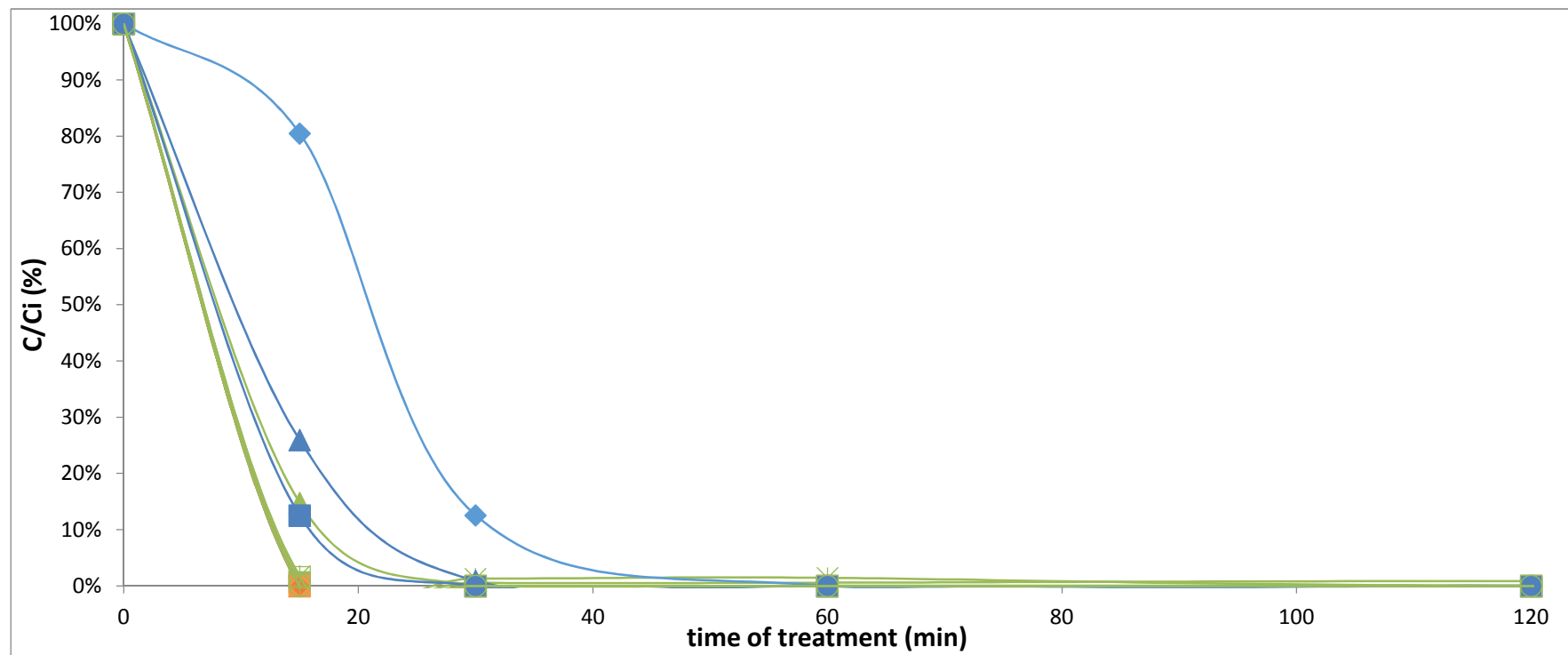


Figure 5S - VOCs degradation profile during the oxidation time for  $O_3/H_2O_2$  process at 40 °C with a dose of 189 g ( $O_3 = 61.5$ ,  $H_2O_2 = 127.5$ ). Solid green squares, toluene; solid green diamonds, ethylbenzene; solid green triangles, 4-methylbenzaldehyde; green crosses, benzene; green stars, 2-ethyl-1-hexanol; empty green triangles, o-xylene; green traces, phenol; empty green circles, 2,6-dimethylphenol; green pluses – 4-ethylphenol; empty green squares, naphthalene; solid blue diamond's 2-nitrophenol; solid blue squares, 2-nitrotoluene; solid blue triangles; solid orange diamonds, di-tert-butyl disulfide; solid orange triangles, 2-ethylthiophene; solid orange squares, dibutyl sulfide.

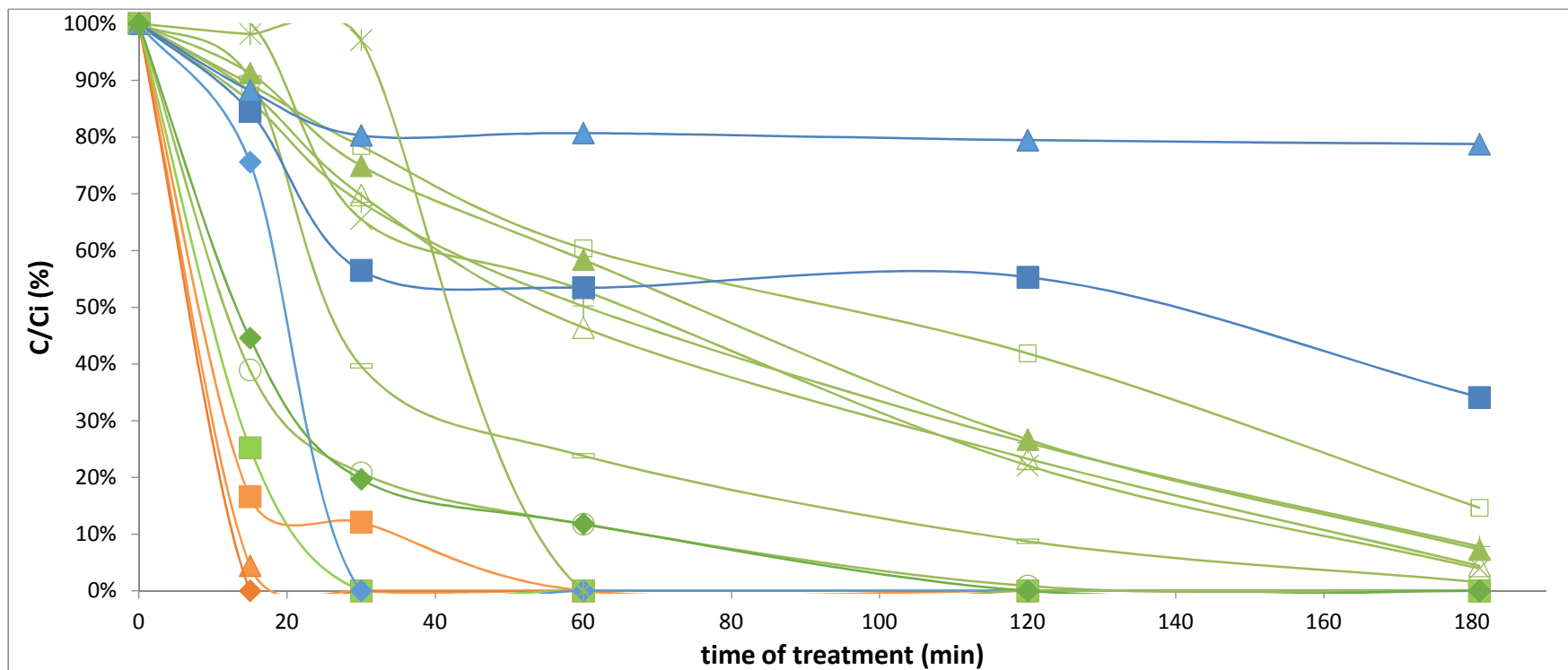


Figure 6S - VOCs degradation profile during the oxidation time for  $\text{Na}_2\text{S}_2\text{O}_8$  process at 40 °C with a dose of 436 g. Empty green squares, toluene; green pluses, ethylbenzene; empty green circles, 4-methylbenzaldehyde; empty green triangles, benzene; green traces, 2-ethyl-1-hexanol; solid green triangles, o-xylene; green crosses, phenol; green stars, 2,6-dimethylphenol; solid green squares, 4-ethylphenol; solid green diamonds, naphthalene; solid blue diamonds 2-nitrophenol; solid blue triangles, 2-nitrotoluene; solid blue squares, nitrobenzene; solid orange diamonds, di-tert-butyl disulfide; solid orange squares, 2-ethylthiophene; solid orange triangles, dibutyl sulfide.



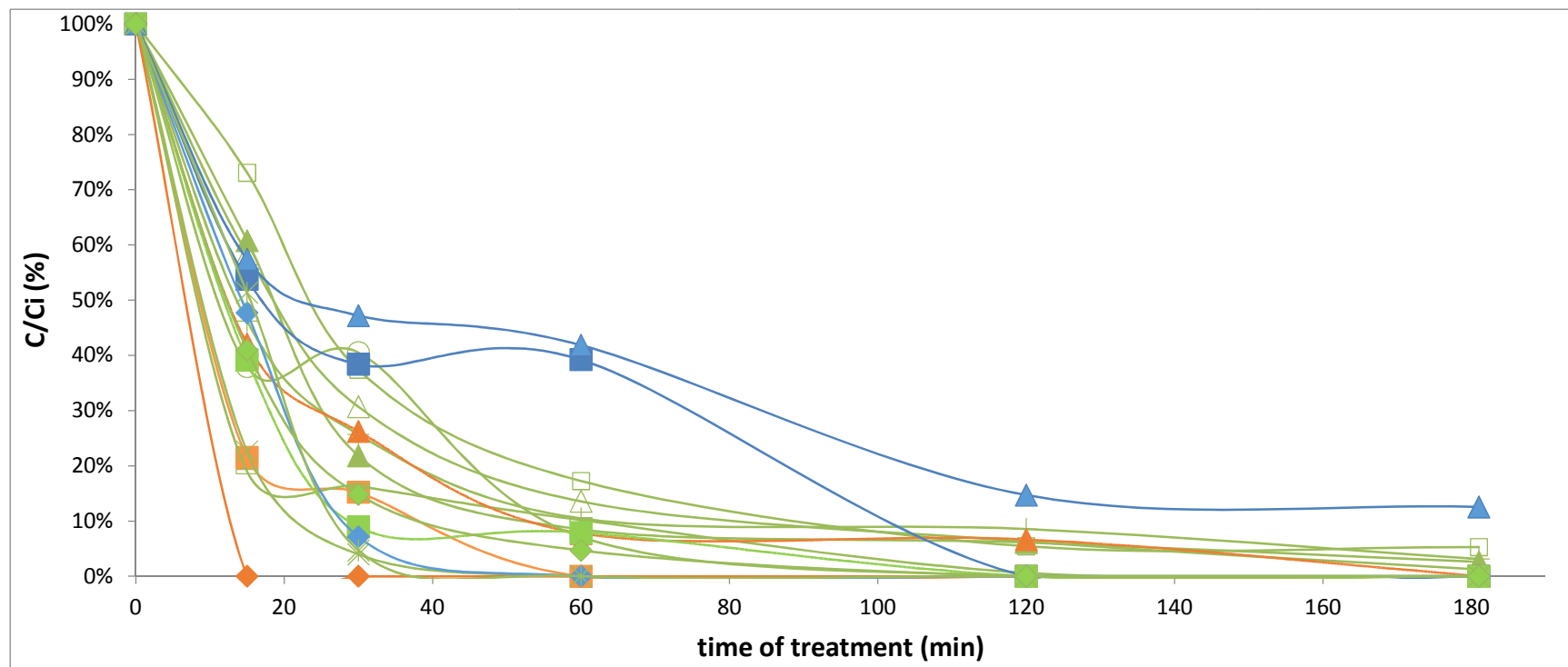


Figure 7S - VOCs degradation profile during the oxidation time for  $\text{Na}_2\text{SO}_8$  process at 60 °C with a dose of 436 g. Empty green squares, toluene; green pluses, ethylbenzene; empty green circles, 4-methylbenzaldehyde; empty green triangles, benzene; green crosses, 2-ethyl-1-hexanol; solid green triangles, o-xylene; green pluses, phenol; green stars, 2,6-dimethylphenol; solid green squares, 4-ethylphenol; solid green diamonds, naphthalene; solid blue diamonds 2-nitrophenol; solid blue triangles, 2-nitrotoluene; solid blue squares, nitrobenzene; solid orange diamonds, di-tert-butyl disulfide; solid orange squares, 2-ethylthiophene; solid orange triangles, dibutyl sulfide.



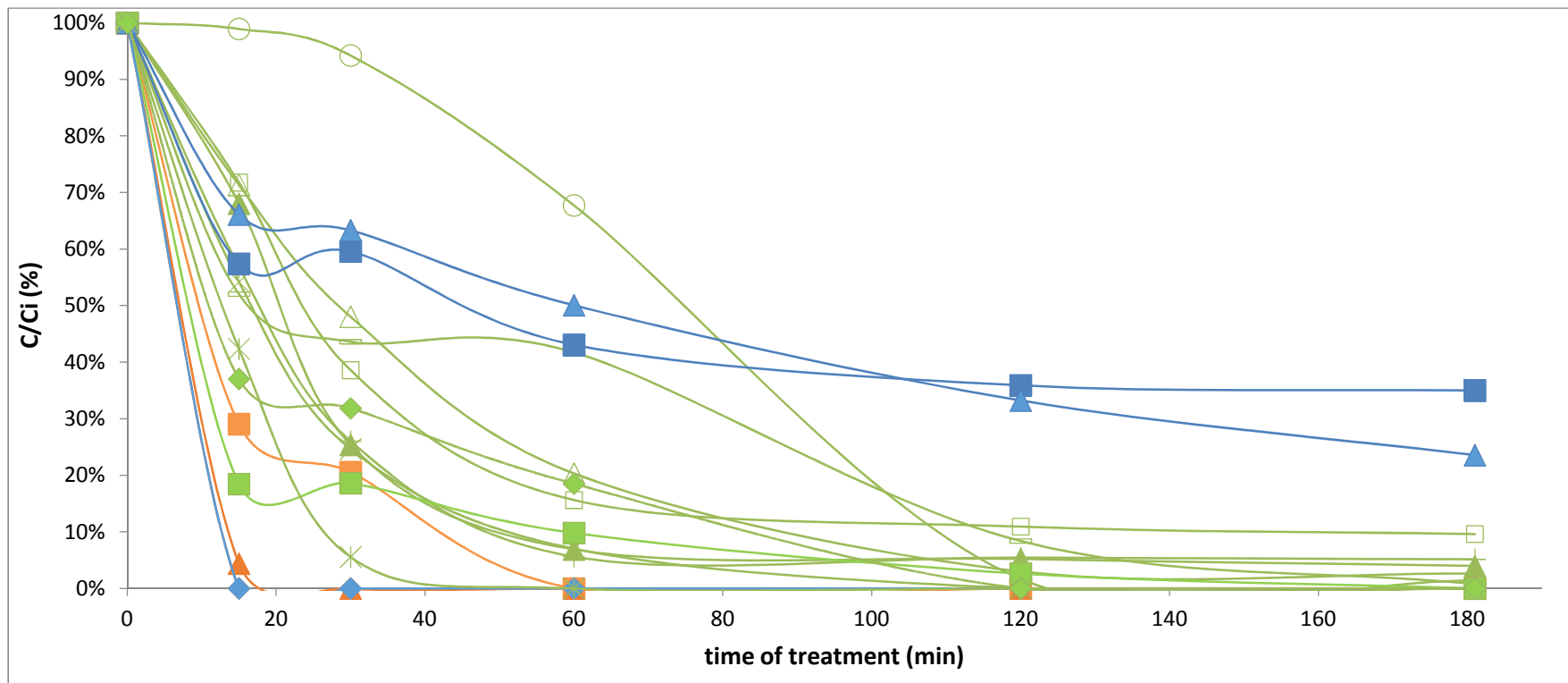


Figure 8S - VOCs degradation profile during the oxidation time for  $\text{Na}_2\text{SO}_8$  process at 60 °C with a dose of 218 g. Empty green squares, toluene; green pluses, ethylbenzene; empty green circles, 4-methylbenzaldehyde; empty green triangles, benzene; green traces, 2-ethyl-1-hexanol; solid green triangles, o-xylene; green crosses, phenol; green stars, 2,6-dimethylphenol; solid green squares, 4-ethylphenol; solid green diamonds, naphthalene; solid blue diamonds 2-nitrophenol; solid blue triangles, 2-nitrotoluene; solid blue squares, nitrobenzene; solid orange diamonds, di-tert-butyl disulfide; solid orange squares, 2-ethylthiophene; solid orange triangles, dibutyl sulfide.



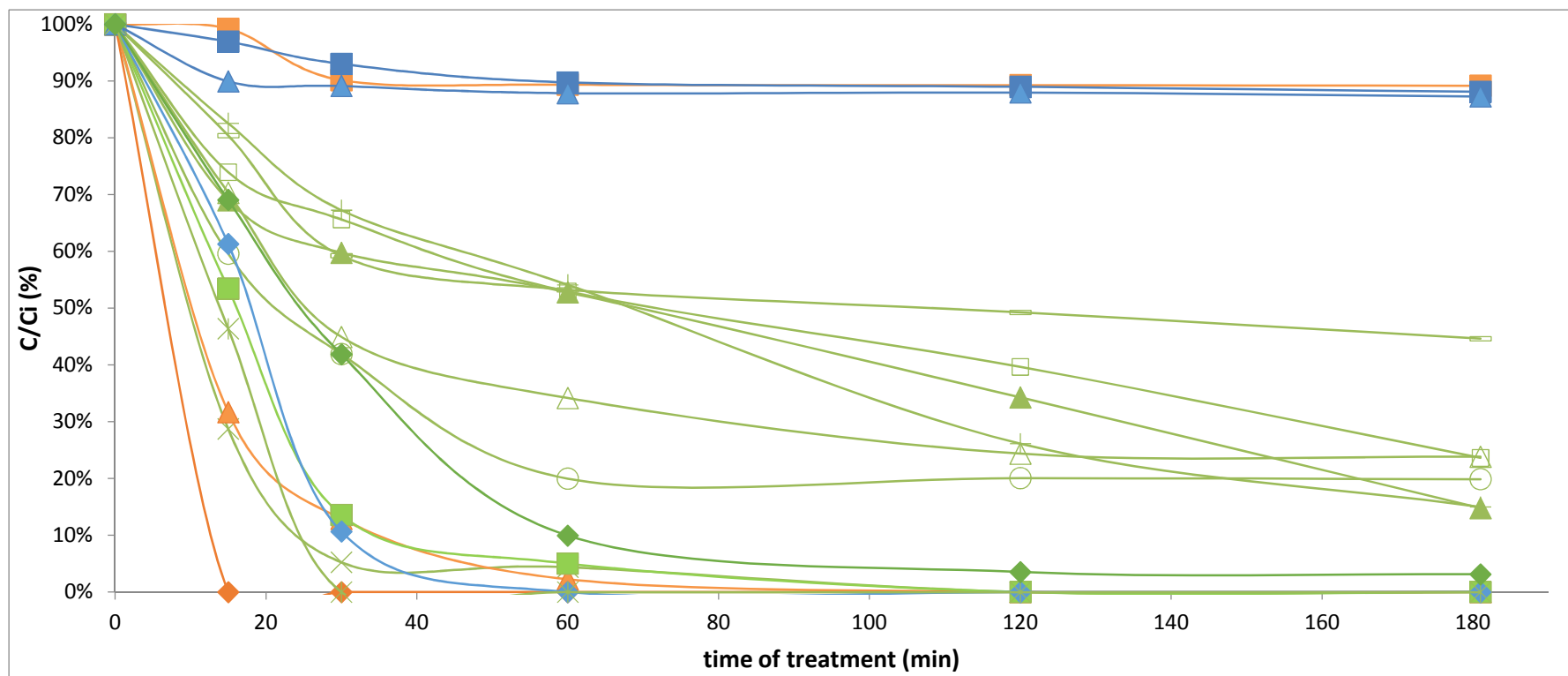


Figure 9S - VOCs degradation profile during the oxidation time for  $\text{KHSO}_5$  process at  $40^\circ\text{C}$  with a dose of 114. g. Empty green squares, toluene; green pluses, ethylbenzene; empty green circles, 4-methylbenzaldehyde; empty green triangles, benzene; green traces, 2-ethyl-1-hexanol; solid green triangles, o-xylene; green crosses, phenol; green stars, 2,6-dimethylphenol; solid green squares, 4-ethylphenol; solid green diamonds, naphthalene; solid blue diamonds 2-nitrophenol; solid blue triangles, 2-nitrotoluene; solid blue squares, nitrobenzene; solid orange diamonds, di-tert-butyl disulfide; solid orange squares, 2-ethylthiophene; solid orange triangles, dibutyl sulfide.



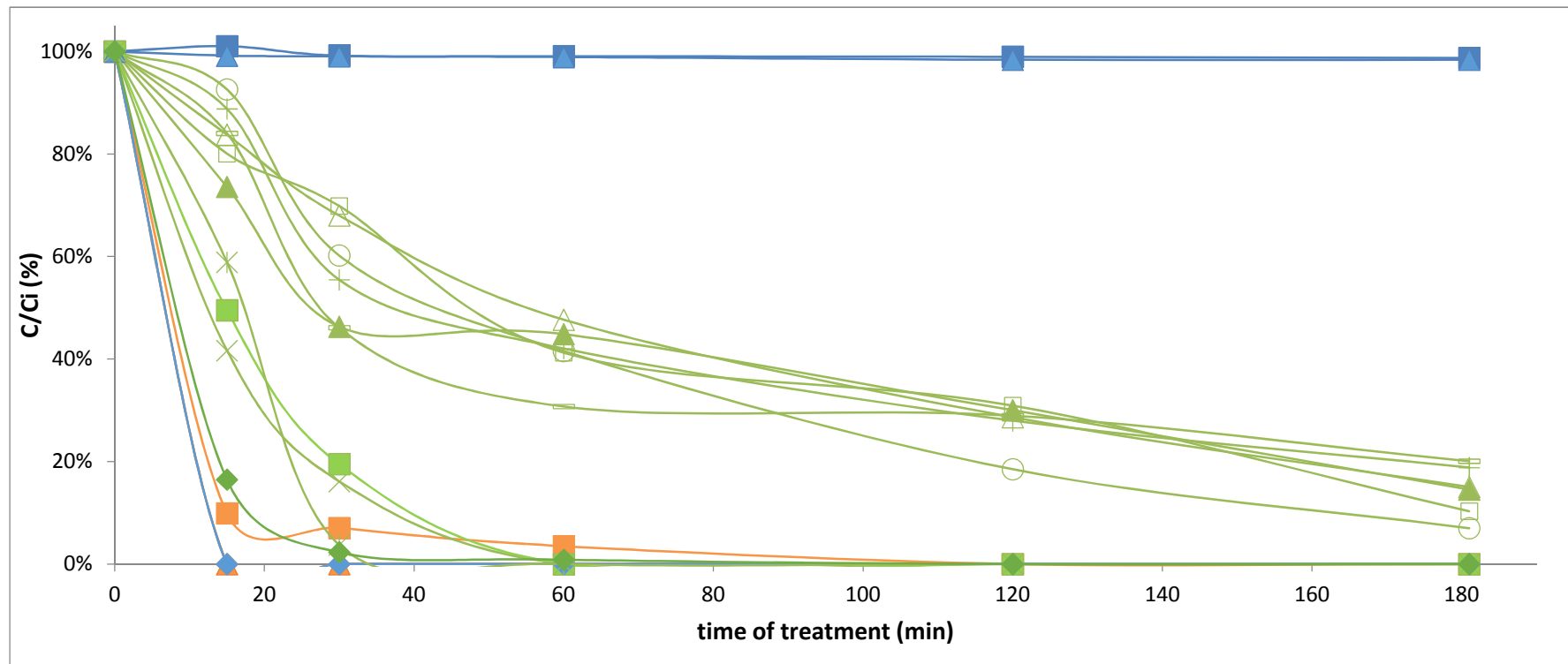


Figure 10S - VOCs degradation profile during the oxidation time for  $\text{KHSO}_5$  process at  $60\text{ }^\circ\text{C}$  with a dose of 114 g. Empty green squares, toluene; green pluses, ethylbenzene; empty green circles, 4-methylbenzaldehyde; empty green triangles, benzene; green traces, 2-ethyl-1-hexanol; solid green triangles, o-xylene; green crosses, phenol; green stars, 2,6-dimethylphenol; solid green squares, 4-ethylphenol; solid green diamonds, naphthalene; solid blue diamonds 2-nitrophenol; solid blue triangles, 2-nitrotoluene; solid blue squares, nitrobenzene; solid orange diamonds, di-tert-butyl disulfide; solid orange squares, 2-ethylthiophene; solid orange triangles, dibutyl sulfide.



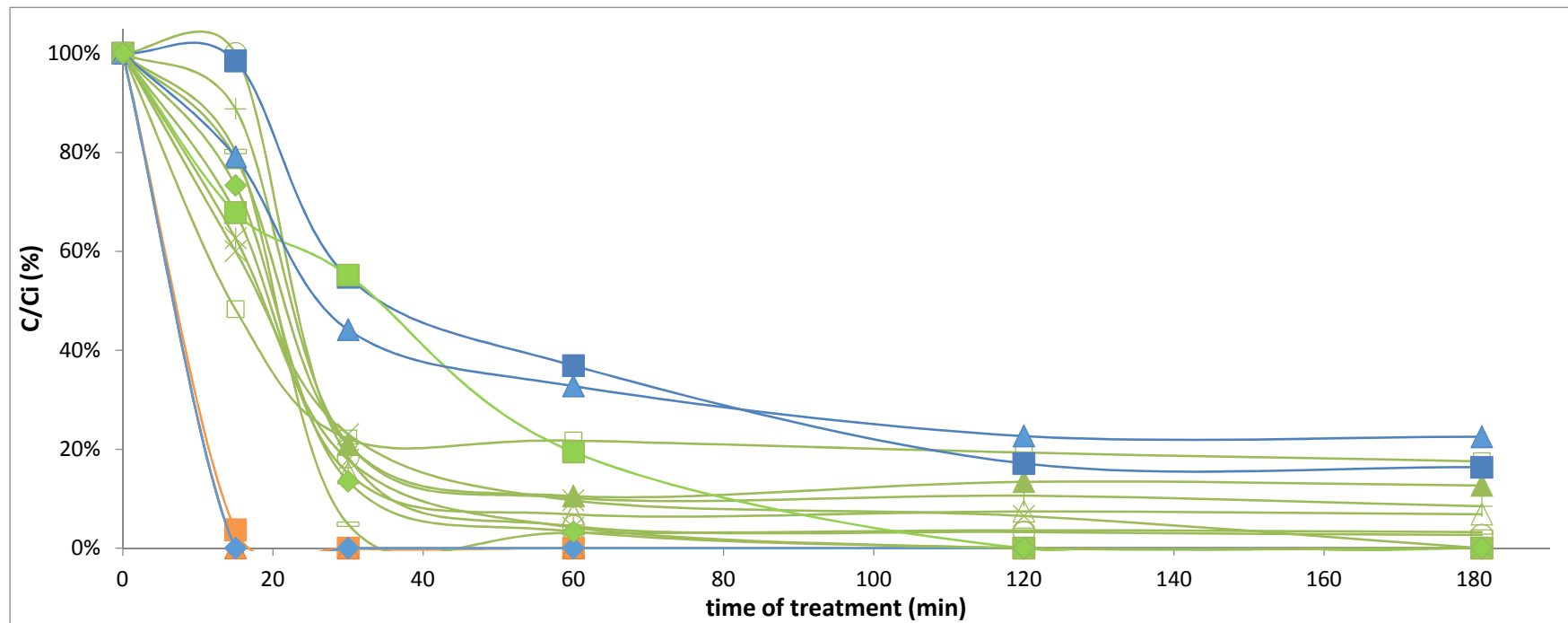


Figure 11S - VOCs degradation profile during the oxidation time for  $\text{KHSO}_5$  process at  $60\text{ }^\circ\text{C}$  with a dose of 70 g. Empty green squares, toluene; green pluses, ethylbenzene; empty green circles, 4-methylbenzaldehyde; empty green triangles, benzene; green traces, 2-ethyl-1-hexanol; solid green triangles, o-xylene; green crosses, phenol; green stars, 2,6-dimethylphenol; solid green squares, 4-ethylphenol; solid green diamonds, naphthalene; solid blue diamonds 2-nitrophenol; solid blue triangles, 2-nitrotoluene; solid blue squares, nitrobenzene; solid orange diamonds, di-tert-butyl disulfide; solid orange squares, 2-ethylthiophene; solid orange triangles, dibutyl sulfide

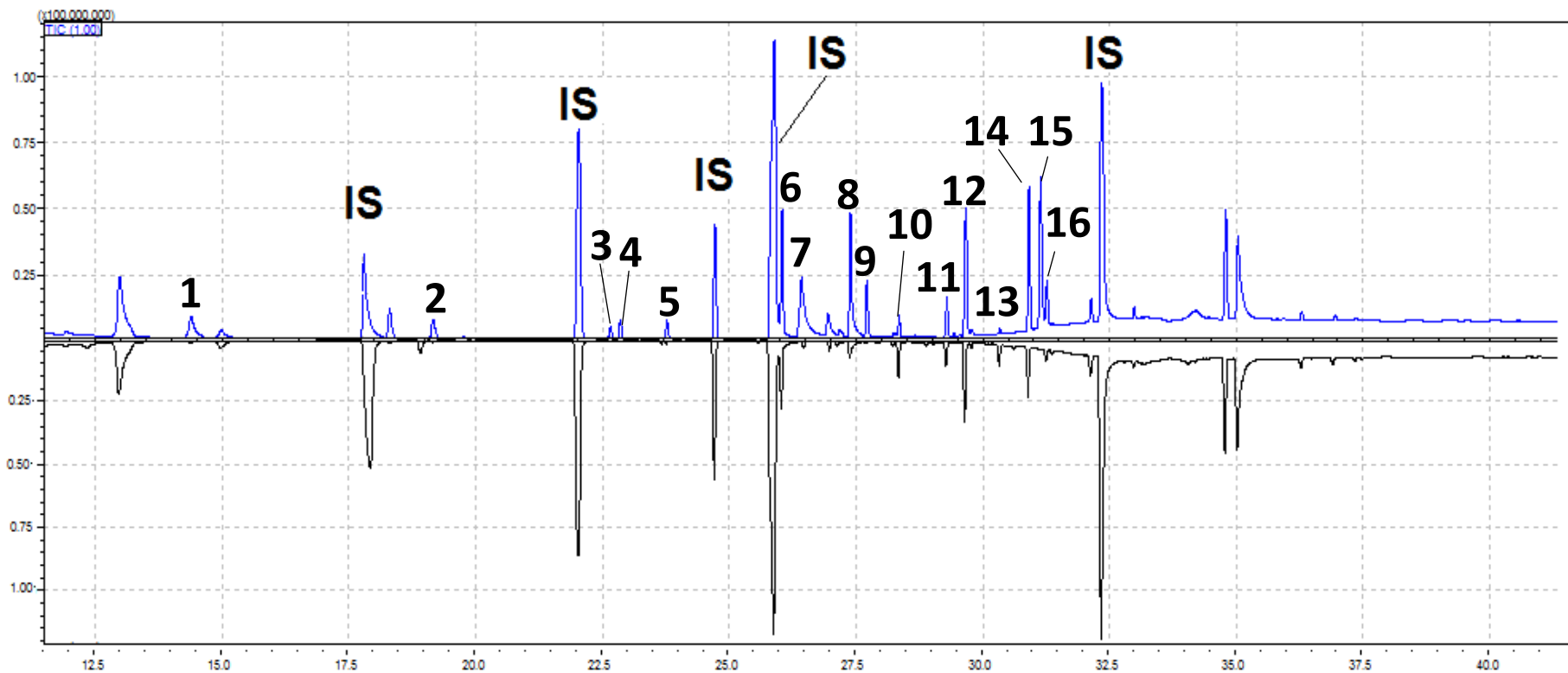


Figure 12S – Chromatogram of the  $\text{H}_2\text{O}_2$  process at 40 °C with an oxidant dose of 62.23 g. Blue line represent the initial sample and the black represents the final sample, after treatment. IS – internal standards; 1 –benzene; 2 – toluene; 3 – ethylbenzene; 4 – ethylthiophene; 5 – o-xylene; 6 – 2-methylcyclohexanone; 7 – 2,4,6 colidine; 8– 2-ethyl-1-hexanol; 9 – phenol; 10 – dibutyl sulfide; 11 – 4-methylbenzaldehyde; 12 – nitrobenzene + 2,6-dimethylphenol; 13 – 2-nitrophenol; 14 – 2-nitrotoluene; 15 – 4-ethylphenol; 16 – naphthalene.

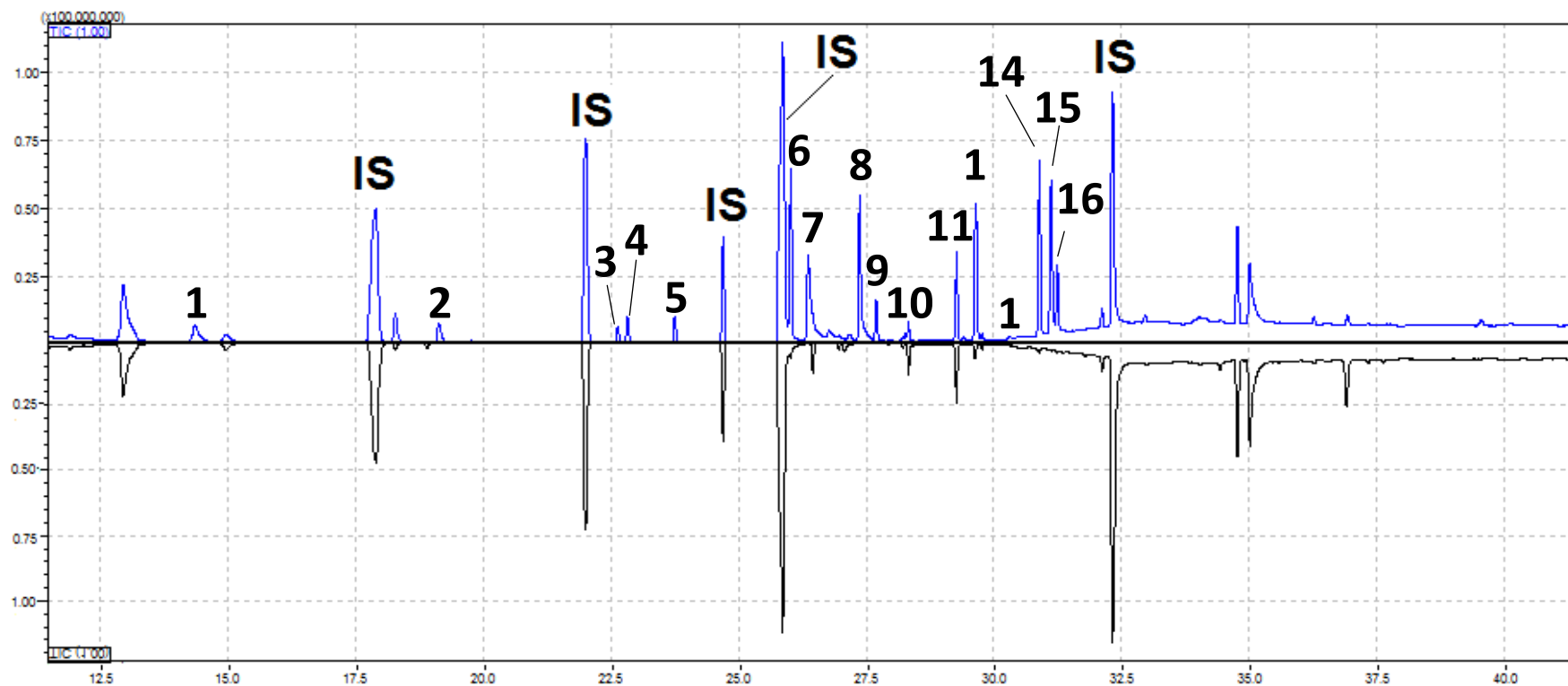


Figure 13S – Chromatogram of the O<sub>3</sub> process at 40 °C with an oxidant dose of 34.69 g. Blue line represent the initial sample and the black represents the final sample, after treatment. IS – internal standards; 1 – benzene; 2 – toluene; 3 – ethylbenzene; 4 – ethylthiophene; 5 – o-xylene; 6 – 2-methylcyclohexanone; 7 – 2,4,6 colidine; 8 – 2-ethyl-1-hexanol; 9 – phenol; 10 – dibutyl sulfide; 11 – 4-methylbenzaldehyde; 12 – nitrobenzene + 2,6-dimethylphenol; 13 – 2-nitrophenol; 14 – 2-nitrotoluene; 15 – 4-ethylphenol; 16 – naphthalene.

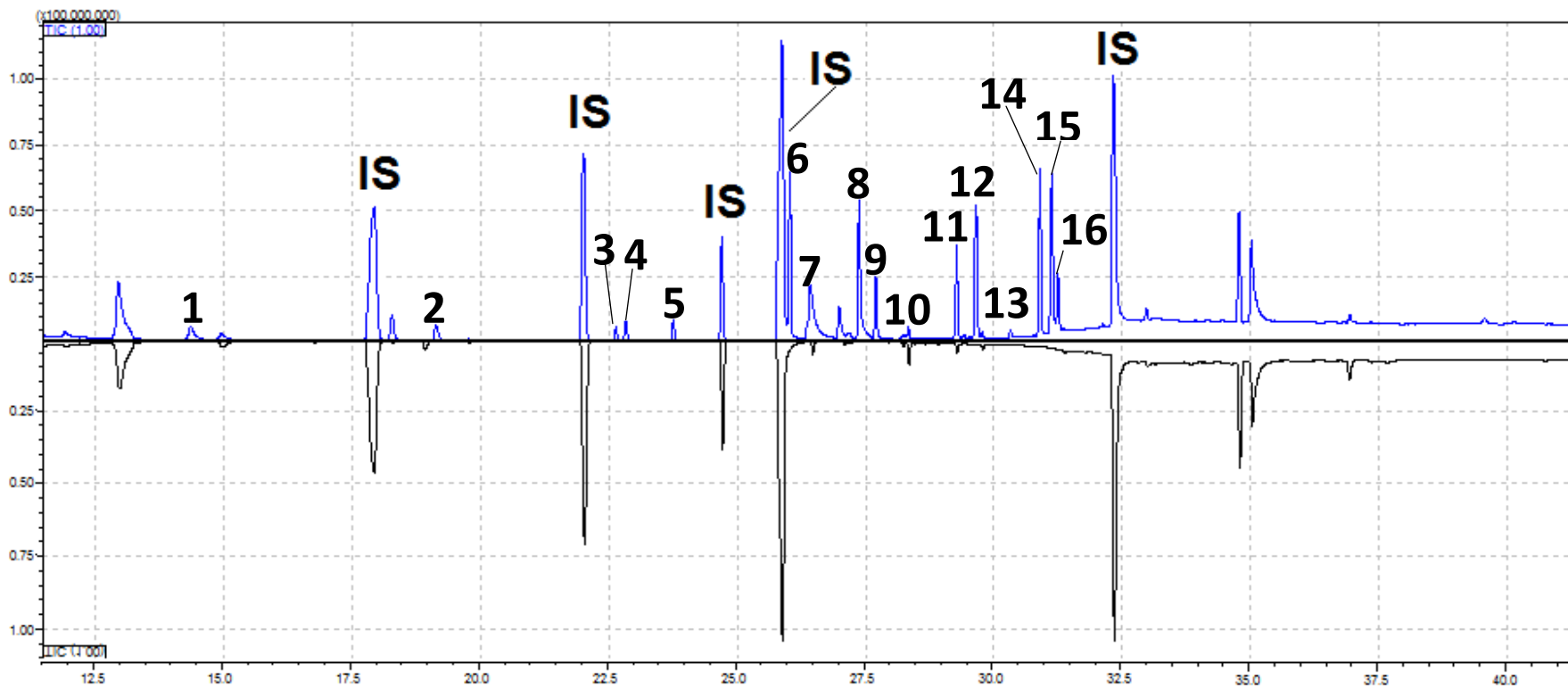


Figure 14S – Chromatogram of O<sub>3</sub> process at 40 °C with an oxidant dose of 69.38 g. Blue line represent the initial sample and the black represents the final sample, after treatment. IS – internal standards; 1 – benzene; 2 – toluene; 3 – ethylbenzene; 4 – ethylthiophene; 5 – o-xylene; 6 – 2-methylcyclohexanone; 7 – 2,4,6 colidine; 8 – 2-ethyl-1-hexanol; 9 – phenol; 10 – dibutyl sulfide; 11 – 4-methylbenzaldehyde; 12 – nitrobenzene + 2,6-dimethylphenol; 13 – 2-nitrophenol; 14 – 2-nitrotoluene; 15 – 4-ethylphenol; 16 – naphthalene.

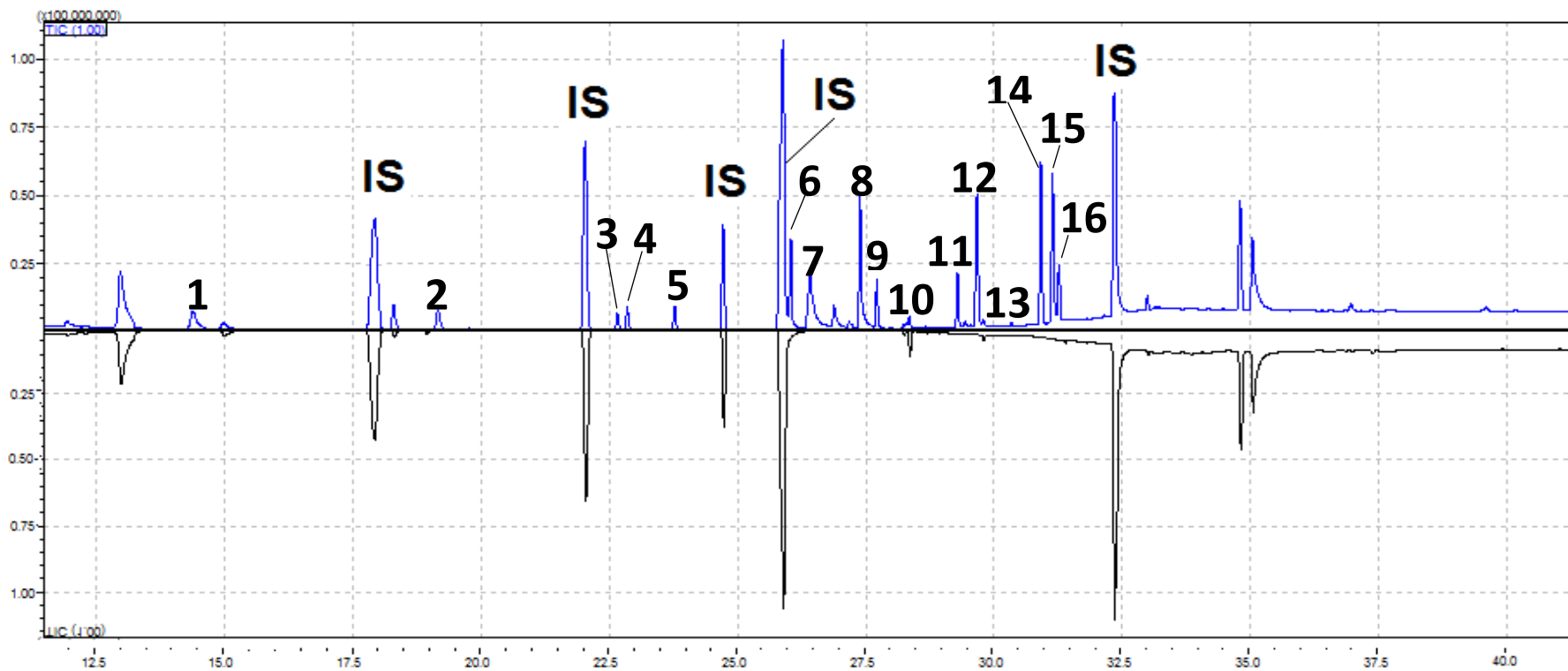


Figure 15S – Chromatogram of  $O_3/H_2O_2$  process at 40 °C with an oxidant dose of 97.9 g. Blue line represent the initial sample and the black represents the final sample, after treatment. IS – internal standards; 1 – benzene; 2 – toluene; 3 – ethylbenzene; 4 – ethylthiophene; 5 – o-xylene; 6 – 2-methylcyclohexanone; 7 – 2,4,6 colidine; 8 – 2-ethyl-1-hexanol; 9 – phenol; 10 – dibutyl sulfide; 11 – 4-methylbenzaldehyde; 12 – nitrobenzene + 2,6-dimethylphenol; 13 – 2-nitrophenol; 14 – 2-nitrotoluene; 15 – 4-ethylphenol; 16 – naphthalene.

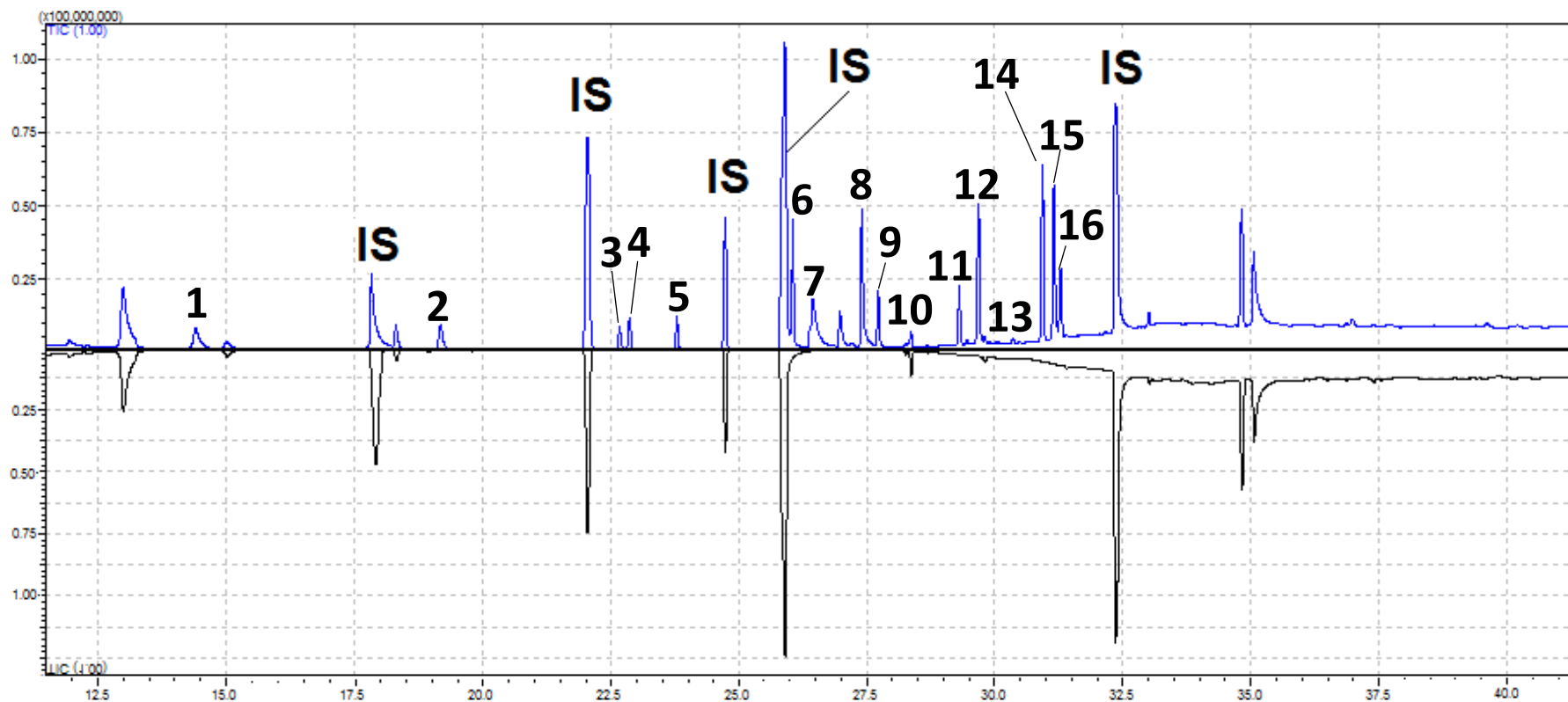


Figure 16S – Chromatogram of  $O_3/H_2O_2$  process at 40 °C with an oxidant dose of 188.8 g. Blue line represent the initial sample and the black represents the final sample, after treatment. IS – internal standards; 1 – benzene; 2 – toluene; 3 – ethylbenzene; 4 – ethylthiophene; 5 – o-xylene; 6 – 2-methylcyclohexanone; 7 – 2,4,6 colidine; 8 – 2-ethyl-1-hexanol; 9 – phenol; 10 – dibutyl sulfide; 11 – 4-methylbenzaldehyde; 12 – nitrobenzene + 2,6-dimethylphenol; 13 – 2-nitrophenol; 14 – 2-nitrotoluene; 15 – 4-ethylphenol; 16 – naphthalene.

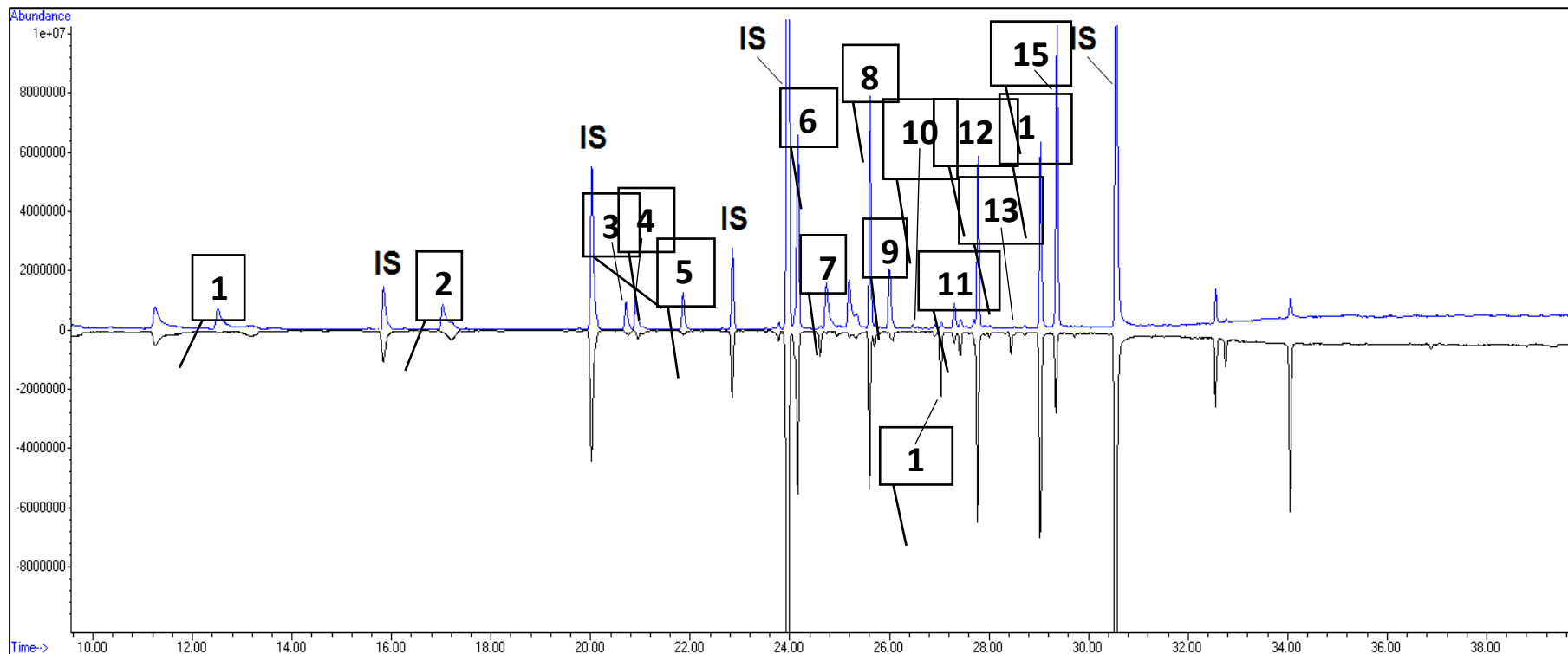


Figure 17S – Chromatogram of  $\text{Na}_2\text{SO}_4$  process at 40 °C with an oxidant dose of 217.79 g. Blue line represent the initial sample and the black represents the final sample, after treatment. IS – internal standards; 1 – benzene; 2 – toluene; 3 – ethylbenzene; 4 – 2-ethylthiophene; 5 – o-xylene; 6 – 2-methylcyclohexanone; 7 – 2,4,6 colidine; 8 – 2-ethyl-1-hexanol; 9 – phenol; 10 – dibutyl sulfide; 11 – 4-methylbenzaldehyde; 12 – nitrobenzene + 2,6-dimethylphenol; 13 – 2-nitrophenol; 14 – 2-nitrotoluene; 15 – 4-ethylphenol + naphthalene; 16 – acetophenone.

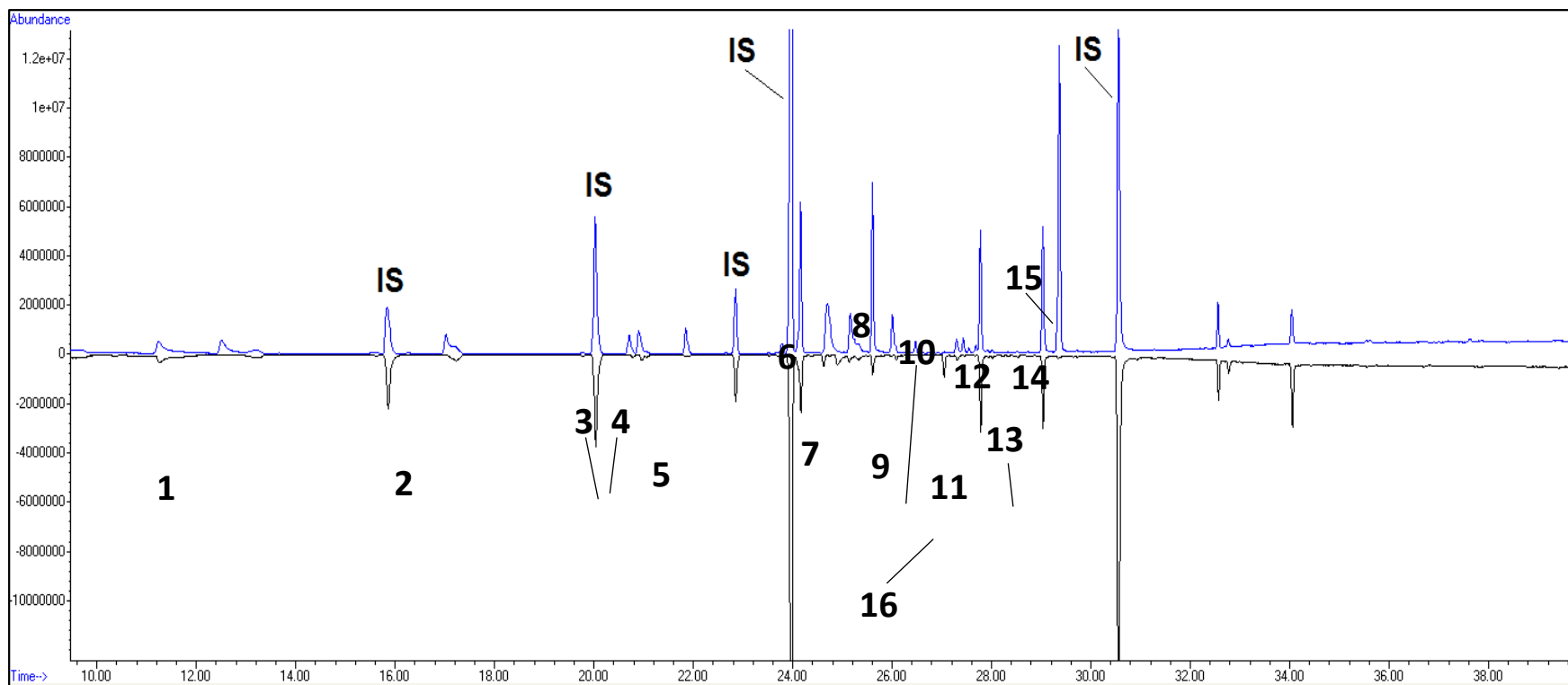


Figure 18S – Chromatogram of  $\text{Na}_2\text{SO}_4$  process at  $40^\circ\text{C}$  with an oxidant dose of 435.39 g. Blue line represent the initial sample and the black represents the final sample, after treatment. IS – internal standards; 1 – benzene; 2 – toluene; 3 – ethylbenzene; 4 – 2-ethylthiophene; 5 – o-xylene; 6 – 2-methylcyclohexanone; 7 – 2,4,6 colidine; 8 – 2-ethyl-1-hexanol; 9 – phenol; 10 – dibutyl sulfide; 11 – 4-methylbenzaldehyde; 12 – nitrobenzene + 2,6-dimethylphenol; 13 – 2-nitrophenol; 14 – 2-nitrotoluene; 15 – 4-ethylphenol + naphthalene; 16 – acetophenone



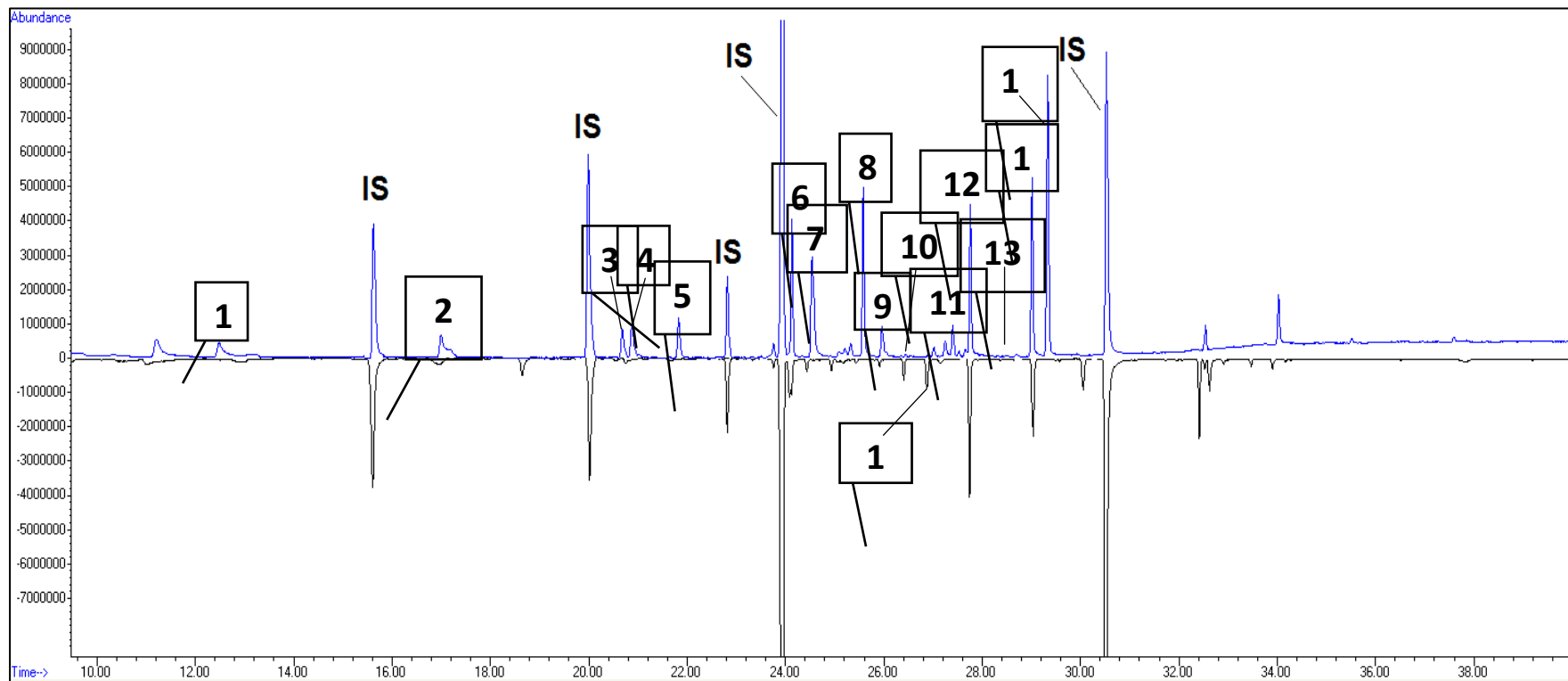


Figure 19S – Chromatogram of  $\text{Na}_2\text{SO}_4$  process at  $60\text{ }^\circ\text{C}$  with an oxidant dose of 217.79 g. Blue line represent the initial sample and the black represents the final sample, after treatment. IS – internal standards; 1 – benzene; 2 – toluene; 3 – ethylbenzene; 4 – 2-ethylthiophene; 5 – o-xylene; 6 – 2-methylcyclohexanone; 7 – 2,4,6 colidine; 8 – 2-ethyl-1-hexanol; 9 – phenol; 10 – dibutyl sulfide; 11 – 4-methylbenzaldehyde; 12 – nitrobenzene + 2,6-dimethylphenol; 13 – 2-nitrophenol; 14 – 2-nitrotoluene; 15 – 4-ethylphenol + naphthalene; 16 – acetophenone.

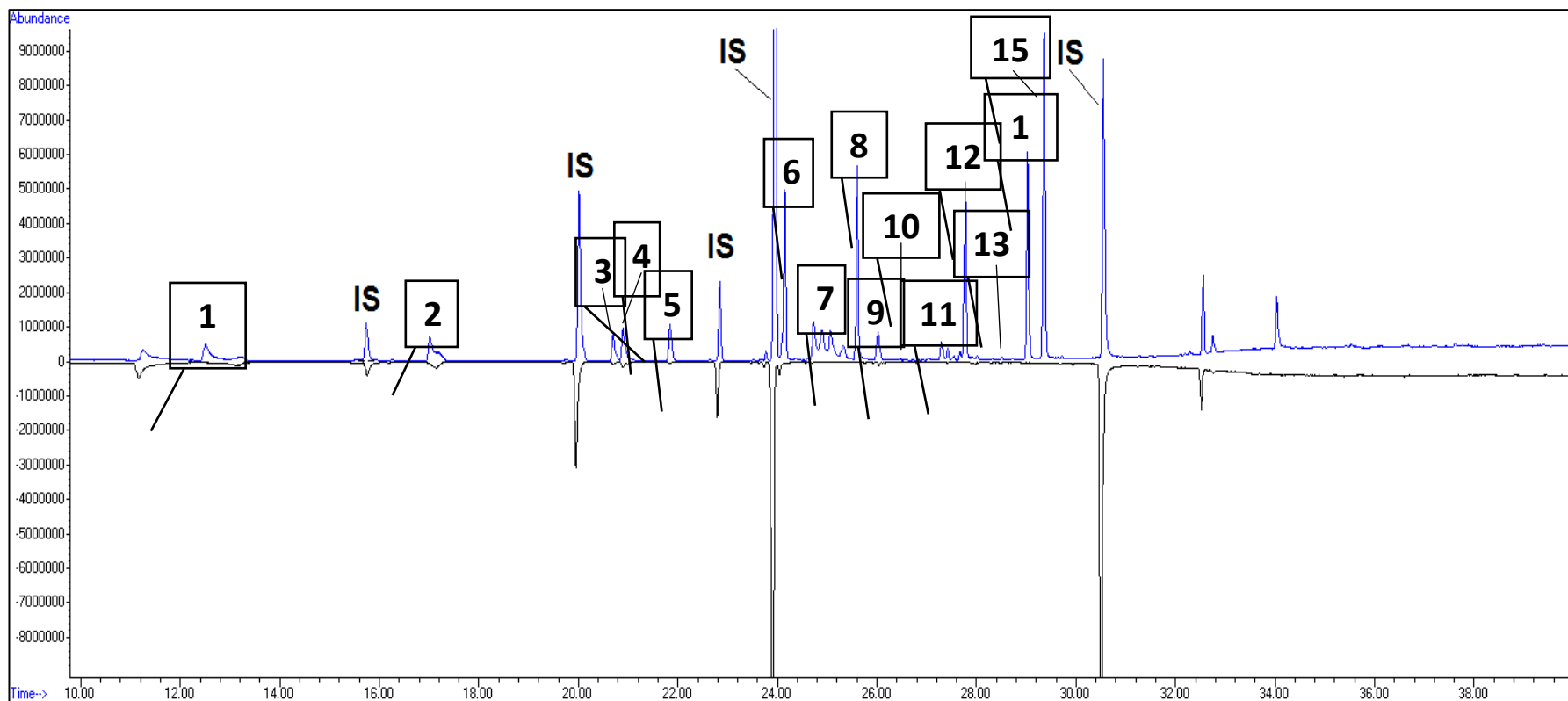


Figure 20S – Chromatogram of  $\text{Na}_2\text{SO}_4$  process at  $60\text{ }^\circ\text{C}$  with an oxidant dose of 435.39 g. Blue line represent the initial sample and the black represents the final sample, after treatment. IS – internal standards; IS – internal standards; 1 – benzene; 2 – toluene; 3 – ethylbenzene; 4 – 2-ethylthiophene; 5 – o-xylene; 6 – 2-methylcyclohexanone; 7 – 2,4,6 colidine; 8 – 2-ethyl-1-hexanol; 9 – phenol; 10 – dibutyl sulfide; 11 – 4-methylbenzaldehyde; 12 – nitrobenzene + 2,6-dimethylphenol; 13 – 2-nitrophenol; 14 – 2-nitrotoluene; 15 – 4-ethylphenol + naphthalene.

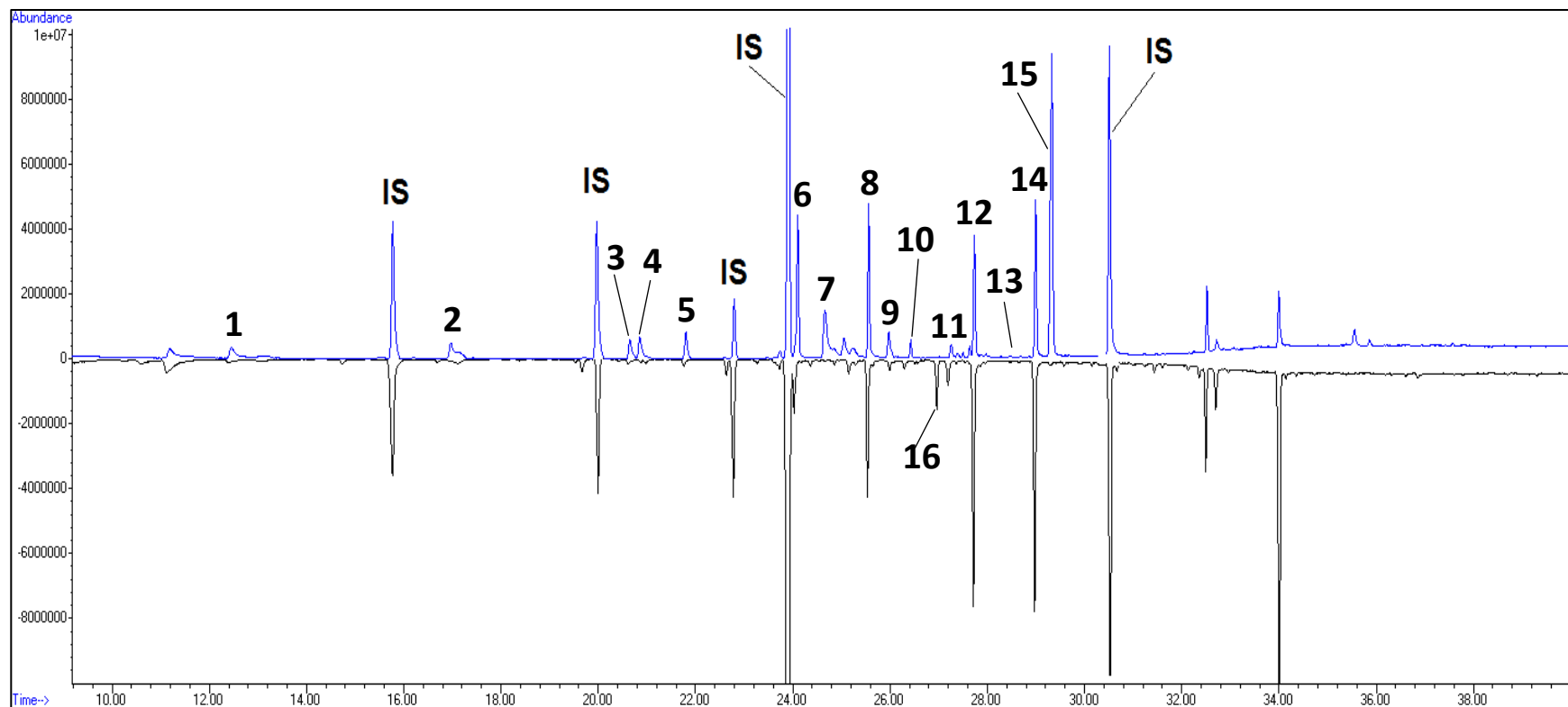


Figure 21S – Chromatogram of  $\text{KHSO}_5$  process at  $40\text{ }^\circ\text{C}$  with an oxidant dose of 114.3 g. Blue line represent the initial sample and the black represents the final sample, after treatment. IS – internal standards; 1 – benzene; 2 – toluene; 3 – ethylbenzene; 4 – 2-ethylthiophene; 5 – o-xylene; 6 – 2-methylcyclohexanone; 7 – 2,4,6 colidine; 8 – 2-ethyl-1-hexanol; 9 – phenol; 10 – dibutyl sulfide; 11 – 4-methylbenzaldehyde; 12 – nitrobenzene + 2,6-dimethylphenol; 13 – 2-nitrophenol; 14 – 2-nitrotoluene; 15 – 4-ethylphenol + naphthalene; 16 – acetophenone.

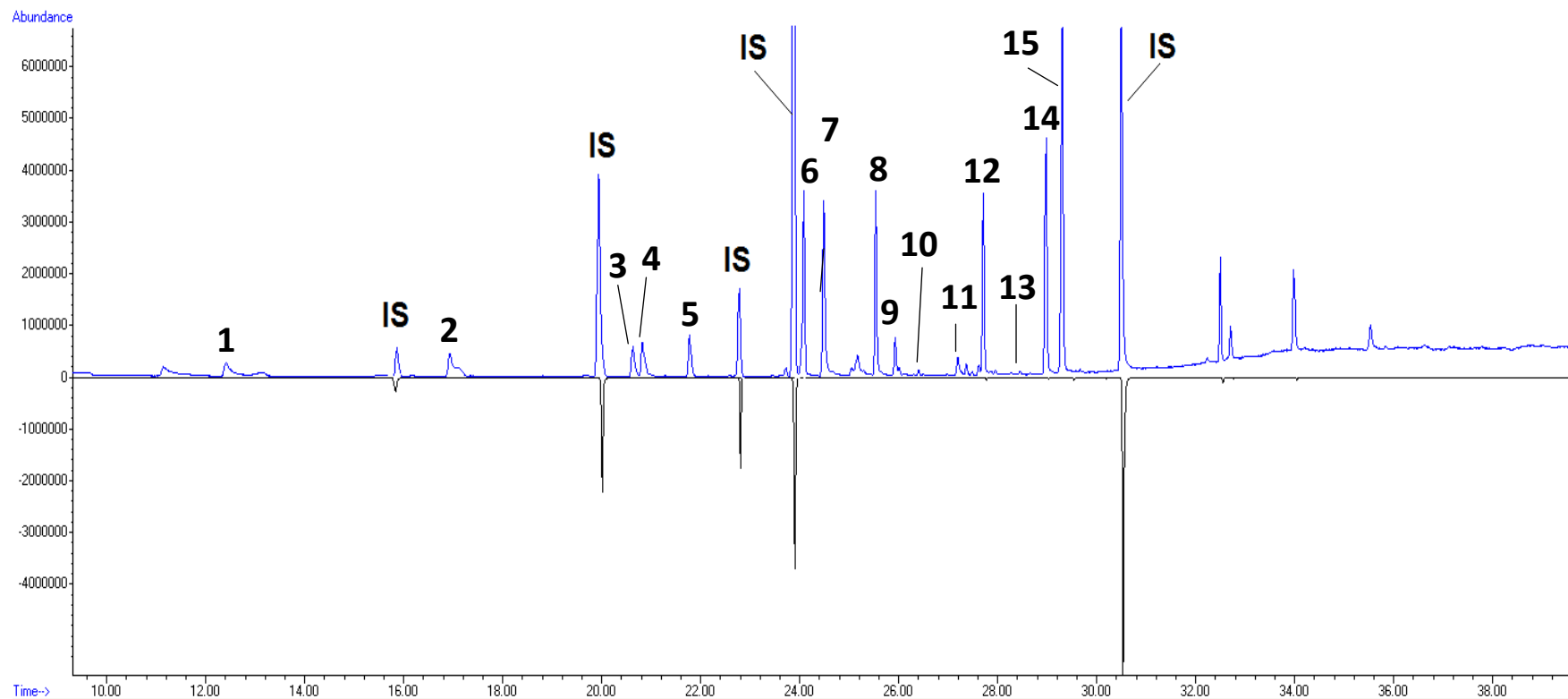


Figure 22S – Chromatogram of  $\text{KHSO}_5$  process at  $60^\circ\text{C}$  with an oxidant dose of 114.3 g. Blue line represent the initial sample and the black represents the final sample, after treatment. IS – internal standards; 1 – benzene; 2 – toluene; 3 – ethylbenzene; 4 – 2-ethylthiophene; 5 – o-xylene; 6 – 2-methylcyclohexanone; 7 – 2,4,6 colidine; 8 – 2-ethyl-1-hexanol; 9 – phenol; 10 – dibutyl sulfide; 11 – 4-methylbenzaldehyde; 12 – nitrobenzene + 2,6-dimethylphenol; 13 – 2-nitrophenol; 14 – 2-nitrotoluene; 15 – 4-ethylphenol + naphthalene.

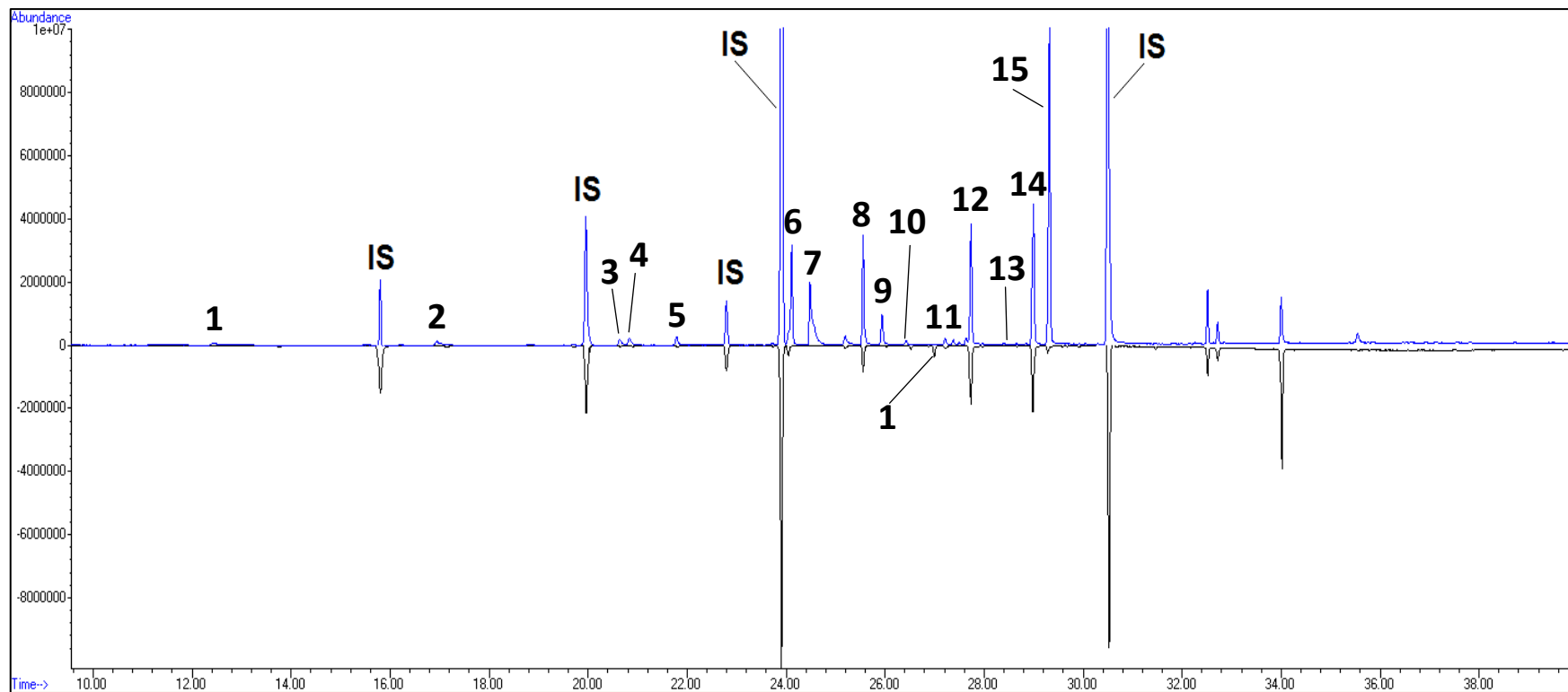


Figure 23S – Chromatogram of  $\text{KHSO}_5$  process at  $40^\circ\text{C}$  with an oxidant dose of 69.67 g. Blue line represent the initial sample and the black represents the final sample, after treatment. IS – internal standards; 1 – benzene; 2 – toluene; 3 – ethylbenzene; 4 – 2-ethylthiophene; 5 – o-xylene; 6 – 2-methylcyclohexanone; 7 – 2,4,6 colidine; 8 – 2-ethyl-1-hexanol; 9 – phenol; 10 – dibutyl sulfide; 11 – 4-methylbenzaldehyde; 12 – nitrobenzene + 2,6-dimethylphenol; 13 – 2-nitrophenol; 14 – 2-nitrotoluene; 15 – 4-ethylphenol + naphthalene; 16 – acetophenone.

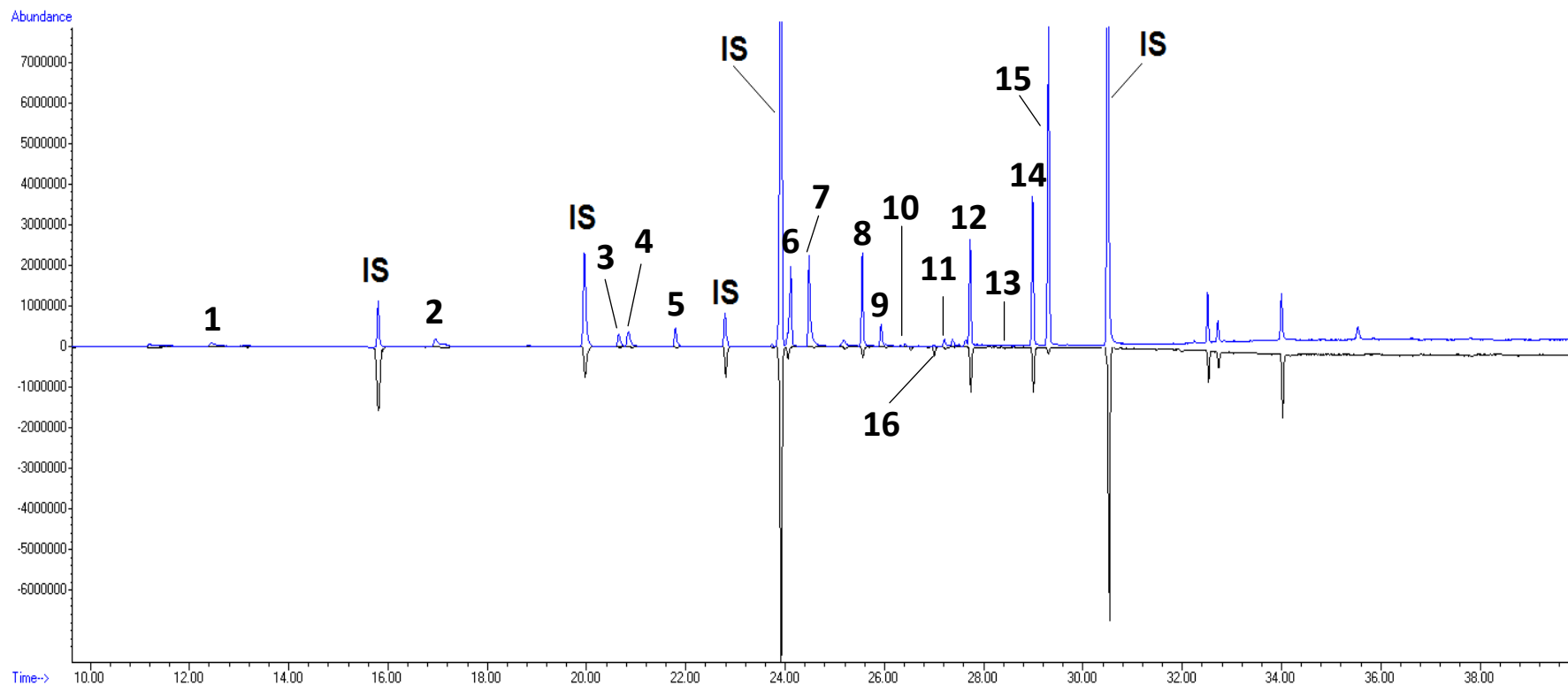


Figure 24S – Chromatogram of KHSO<sub>5</sub> process at 60 °C with an oxidant dose of 69.67 g. Blue line represent the initial sample and the black represents the final sample, after treatment. IS – internal standards; 1 – benzene; 2 – toluene; 3 – ethylbenzene; 4 – 2-ethylthiophene; 5 – o-xylene; 6 – 2-methylcyclohexanone; 7 – 2,4,6 colidine; 8 – 2-ethyl-1-hexanol; 9 – phenol; 10 – dibutyl sulfide; 11 – 4-methylbenzaldehyde; 12 – nitrobenzene + 2,6-dimethylphenol; 13 – 2-nitrophenol; 14 – 2-nitrotoluene; 15 – 4-ethylphenol + naphthalene; 16 – acetophenone.